

1 Advection and in situ processes as drivers of change for the abundance of large
2 zooplankton taxa in the Chukchi Sea

3

4 Adam Spear*, Jeff Napp, Nissa Ferm, David Kimmel

5

6 *Alaska Fisheries Science Center, National Marine Fisheries Service, National Oceanic and Atmospheric*
7 *Administration, 7600 Sand Point Way NE, Seattle, WA 98115-6349, USA*

8

9 *Corresponding author.

10 *E-mail address:* Adam.Spear@noaa.gov (A. Spear)

11 **Keywords:** Zooplankton, Euphausiids, Climate, Chukchi Sea, Sea ice, Arctic food webs

12

13 **ABSTRACT**

14 The Chukchi Sea has recently experienced increased water temperatures, increased advection of
15 water from the Bering Sea, declines in sea-ice concentration, and shorter periods of ice coverage.
16 These physical changes are expected to impact trophic food-webs and ecosystem attributes. In
17 this study, a series of research surveys were conducted in the summers of 2011-2015 to
18 characterize the physical environment and its relation to the abundance of large zooplankton.
19 Large zooplankton are key prey for many higher trophic level organisms including seabirds,
20 marine mammals, and fishes. Yearly advection from the Bering Sea influenced the adult large

21 zooplankton abundance, but this influence was less apparent in the earlier development stages.
22 Known development times of stages of zooplankton, along with their location within the study
23 area, suggested that a fraction of the zooplankton standing stock was the result of local
24 production. Decreased advection and later ice retreat resulted in higher abundances of the lipid-
25 rich copepod *Calanus glacialis*. Warmer conditions with increased advection from the Bering
26 Sea resulted in higher abundances of euphausiids. Warming, sea-ice melting, and increases in
27 transport of Bering Sea water and plankton into the Chukchi Sea are ongoing, and changes in
28 food-web structure are likely to result.

29

30 **1. Introduction**

31

32 The zooplankton of the Chukchi Sea shelf consist of taxa that are more similar to the
33 Pacific Ocean community than the Arctic Ocean community (Ashjian et al., 2010; Hopcroft et
34 al., 2010; Eisner et al., 2013; Questel et al., 2013; Ashjian et al., 2017; Pinchuk and Eisner,
35 2017), a result of the transport of North Pacific water through the Bering Strait into the Arctic.
36 Northward advection through the Bering Strait combines several water masses that results in the
37 transport of relatively warm, nutrient-rich water, as well as primary and secondary producers into
38 the Arctic (Woodgate et al., 2005; Gong and Pickart, 2015; Danielson et al., 2017; Stabeno et al.,
39 2018). Northward advection through the Bering Strait in the summer, along with sea-ice melting
40 and episodic upwelling from the Beaufort Sea on to the shelf and Barrow Canyon, results in a
41 highly productive and complex shelf ecosystem that responds to local, regional and global
42 forcing (e.g. Bond et al., 2019). Adding to the complexity of the Chukchi Sea shelf ecosystem,
43 recent reports have shown dramatic changes in timing and extent of sea-ice coverage, along with

44 considerable increases in sea surface temperatures (National Snow and Ice Data Center, nsidc.org;
45 Timmermans and Ladd, 2019; Perovich et al., 2019).

46 In summer, the northern Bering and Chukchi seas experience increased day length and
47 melting sea ice, resulting in a phytoplankton bloom. The bulk of the bloom sinks to the bottom
48 due to the shallow depth (< 50 m) and relatively low grazing impact on phytoplankton (Campbell
49 et al., 2009), supporting a robust benthic community. Recent studies, however, have shown a
50 temporal decrease in benthic biomass in the northern Bering Sea, suggesting a possible
51 weakening of benthic-pelagic coupling as the ice retreat now occurs earlier in the season
52 (Grebmeier, 2006a; Grebmeier, 2006b; Grebmeier, 2012). Concurrently, zooplankton biomass in
53 the Chukchi Sea has increased over the past seven decades (Ershova et al., 2015), which can be
54 explained, in part, by increasing temperatures, reduction in sea ice, and an increase in northward
55 water transport through the Bering Strait (Ershova et al., 2015; Woodgate et al., 2015;
56 Woodgate, 2018). These trends suggest a potential ecosystem regime shift is underway in the
57 Pacific Arctic, with consequences for local food webs. These changes emerge from both direct
58 and indirect effects on both the indigenous biota residing in the ecosystem as well as the
59 introduced species. Changes in the timing and type of production within the pelagic and benthic
60 communities, will result in changes in benthic-pelagic coupling that have the potential to effect
61 higher trophic levels such as birds, marine mammals, fish, and the people who live in the region.

62 One specific taxon of interest for our studies were bowhead whales (*Balaena mysticetus*)
63 that forage as they migrate southwestward in the fall through the Utqiagvik (formerly known as
64 Barrow) region from the Beaufort Sea (Moore et al., 2010; Quakenbush et al., 2010; Citta et al.,
65 2012). Studies have reported improvements in bowhead body condition in association with
66 earlier ice retreat and increase in the area of open water (George et al., 2015). The observed

67 improvements in bowhead body condition may be the result of increased prey populations,
68 specifically euphausiids and copepods that dominate the prey in stomachs of bowhead whales
69 harvested near Utqiagvik, Alaska (Lowry et al., 2004; Ashjian et al., 2010; Moore et al., 2010;
70 George et al., 2015). Previous studies suggested that euphausiids are advected along the bottom
71 from the northern Bering Sea into the Chukchi Sea, and subsequently concentrated into dense
72 aggregations through upwelling onto the Beaufort Sea shelf towards Barrow Canyon (Berline et
73 al., 2008; Ashjian et al., 2010). Zooplankton sampling in the Chukchi Sea has generally
74 underestimated populations of euphausiids because estimates were based on collections from
75 small (0.25-0.6 cm diameter) aperture size plankton bongo nets (Hopcroft et al., 2010; Eisner et
76 al., 2013; Questel et al., 2013; Ashjian et al., 2017; Pinchuk and Eisner, 2017) and because the
77 predominantly daytime vertical or oblique sampling failed to target krill layers near the bottom
78 (Coyle and Pinchuk, 2002).

79 The main objectives of this study were 1) to understand the transport pathways of
80 euphausiids from the Bering Strait to Barrow Canyon, 2) evaluate the abundance of other large
81 planktonic prey for whales in the region, and 3) provide data on the status and trends of Chukchi
82 Sea zooplankton communities. This study builds on other research based on conceptualized
83 modeling to explain the dynamics of late-summer euphausiid populations in this region (Berline
84 et al., 2008; Ashjian et al., 2010) by providing empirical data collected from epibenthic and
85 plankton tows that should more accurately reflect the abundance of euphausiid and other
86 epibenthic taxa. We compared epibenthic and pelagic zooplankton abundances to assess whether
87 they were significantly different and to explore whether epibenthic tows were a more accurate
88 reflection of near-bottom taxa. We hypothesized that advection of zooplankton from the Bering
89 Sea to be the main driver of zooplankton abundance in the region. To test this, we compared

90 zooplankton abundance across years and locations, and calculated krill development times to see
91 if euphausiids captured in this study could have reached that stage after having been advected
92 from the Bering Sea.

93

94

95 **2. Methods**

96

97 *2.1. Study area*

98

99 The Chukchi Sea has a broad, mostly shallow (<50 m) shelf situated between Alaska and
100 Siberia (Fig. 1). Survey transects varied among years, 2011 – 2015, depending on the scientific
101 focus for the year, available ship time, and ice distribution. Surveys were conducted in the late
102 summer, lasting approximately 30 days (~August 5th – September 5th), except for 2014, which
103 was September 22nd – October 12th. For analysis and description purposes, the study area was
104 divided into ‘Beaufort’, ‘Southwest,’ ‘Central,’ and ‘Northeast’ regions that are established from
105 statistically different oceanographic conditions (Eisner et al., 2012; Randall et al., 2019).

106

107 *2.2. Physical data*

108

109 Hydrographic data, including temperature and salinity, were collected using a SBE
110 911plus and FastCAT SBE 49 systems (SeaBird Electronics). Sea Surface temperatures (SST)
111 were averaged from 5 – 10 m depth. We quantified broad-scale patterns in sea-ice concentration
112 using satellite data. Sea-ice concentration (percentage of ocean covered by sea-ice) and extent

113 data were obtained after the surveys from a Scanning Multichannel Microwave Radiometer
114 (SMMR) on the Nimbus-7 satellite and from the Special Sensor Microwave/Imager (SSM/I)
115 sensors on the Defense Meteorological Satellite Program's (<https://nsidc.org>; Comiso, 1999).
116 Bering Strait volume transport data were acquired from moored Acoustic Doppler Current
117 Profiler (ADCP) measurements (Woodgate et al., 2015; Woodgate, 2018). Northeastward water
118 column volume transport, in Sverdrups (Sv), was calculated according to Stabeno et al. (2018)
119 from current data measured at C1, C2, and C3 moorings along the Icy Cape transect. Transport
120 was averaged over 14 and 30 days leading up to the date that the station was sampled.

121

122 *2.3. Zooplankton net data*

123

124 Zooplankton were collected primarily during daylight hours using a multiple-opening and
125 closing 1 m² Tucker Sled trawl equipped with a FastCAT, and sled-like runners at the bottom so
126 that samples could be taken in close proximity to the bottom. A 505 µm (2013-2015) or a 333
127 µm (2011-2012) mesh net sampled while the sled was towed at a speed of 1.5-2.0 knots along
128 the bottom for 2 minutes, then mechanically tripped to close and simultaneously open a second
129 net to sample the entire water column from the bottom to the surface (wire retrieval rate 20 m
130 min⁻¹). For smaller taxa, a 25 cm net with 150 µm mesh was suspended in the larger net that
131 profiled the entire water column. Note that this setup is not ideal in cases where clogging in the
132 20- cm net occurs, thus the possibility of inaccurate volume filtered readings exist in this study.
133 Samples that appeared questionable (e.g. low flowmeter readings, large jellyfish in the net) were
134 excluded from the analysis. Smaller taxa such as *C. glacialis* and euphausiid furcilia were
135 enumerated in the water column only and not in the epibenthic samples. Both Tucker nets were

136 equipped with a separate calibrated General Oceanics flow meter to estimate volume filtered.
137 Plankton captured by the nets were washed into the cod-ends, sieved through appropriately-sized
138 wire mesh screens and preserved in glass jars with sodium borate-buffered 5% Formalin.
139 Samples were inventoried at the end of the cruise and then sent to the Plankton Sorting and
140 Identification Center in Szczecin, Poland, for processing. Subsampled taxa were enumerated and
141 identified to lowest possible genera and life stage and returned to the Alaska Fisheries Science
142 Center for verification. Ten percent of the returned samples were checked for quality
143 assurance/quality control of species identification and enumeration.

144

145 *2.4. Zooplankton data analysis*

146

147 Zooplankton abundance was reported as four general categories in the context of known
148 bowhead whale prey in the region (Lowry et al., 2004; Moore et al., 2010), including:
149 euphausiids (primarily *Thysanoessa raschii*), amphipods (dominant species included *Themisto*
150 *libellula* and unidentified Gammaridea), mysids (dominant species included *Neomysis rayii* and
151 *Pseudomma truncatum*), and copepods (*Calanus glacialis*). Analysis of variance (ANOVA) was
152 used to examine epibenthic and pelagic variation across years in *T. raschii*, mysid, and amphipod
153 abundance.

154 Development times of *Thysanoessa* spp. stages were estimated using the formula:

$$155 \quad R_2 = R_1 * Q_{10}^{\frac{T_2 - T_1}{10}}$$

156 where R_1 and R_2 are the development rates (d^{-1}) at temperature T_1 and T_2 ($^{\circ}C$), respectively
157 (Tegllhus et al., 2015). We used the Q_{10} of 2.04 (Pinchuk and Hopcroft, 2006). The calculated
158 temperature (T_2) and development rate (R_2) were normalized to 5 $^{\circ}C$ and 0.016 d^{-1} (for furcilia;

159 0.045 d⁻¹ for calyptopis), obtained from Teglhus et al. (2015). We chose the measured rates from
160 Teglhus et al. (2015) because of the similar temperature conditions (5-8° C) and because a mixed
161 population of krill was used as we also have a mixed community. These were also the slowest
162 known development rates for *Thysanoessa* spp. furcilia compared to previous studies (see Table
163 3 in Teglhus et al., 2015); this prevented an overestimation of development rates of *Thysanoessa*
164 spp. under conditions that may be significantly influenced by availability of food such as
165 phytoplankton (Pinchuk and Hopcroft, 2007). Development times were then compared to
166 satellite-tracked drifter data (Stabeno et al., 2018) to explore the possibility of recent
167 reproduction in the Chukchi Sea.

168 We used the mgcv package (Wood, 2011) in R (R Core Team, 2019) to fit generalized
169 additive models (GAM) with Gaussian distribution to relate changes in C2 and C5 stages of *C.*
170 *glacialis*, *T. raschii* (adult and juvenile), and euphausiid furcilia mean abundance to
171 environmental variables. These two particular stages in each species were chosen to contrast
172 different ages, with C2 representing younger and C5 representing older *C. glacialis*, and furcilia
173 representing younger and adults/juveniles representing older *T. raschii*. For simplicity, we
174 excluded stages C3 and C4 from the analysis as these stage abundances are correlated to the C5
175 stage (data not shown). We chose to exclusively use epibenthic abundances of *T. raschii* since
176 most of our sampling occurred primarily during the day and when the vast majority of
177 euphausiids would be at or near the bottom. Restricted Maximum Likelihood (REML) method
178 was used as the smoothing parameter estimation. The model selection was done by assessing
179 deviance explained, R^2 , and Akaike information criterion (AIC). Residuals were analyzed to
180 ensure there were no obvious deviations from normal distributions, and we examined the
181 response versus. fitted value for patterns. We assessed ten environmental variables for inclusion

182 in the GAMs including: latitude, longitude, bottom temperature, surface temperature, bottom
183 salinity, surface salinity, 14 and 30-day northeastward transport, year, and day of the year
184 (hereinafter referred to as ordinal day).

185

186

187 **3. Results**

188

189 *3.1. Environmental Conditions*

190

191 Sea surface temperatures (SST) were warmest in 2011 (mean SST 6.89 ± 1.35 °C) and
192 coldest in 2013 (mean SST 2.64 ± 2.61 °C). Both 2012 (mean SST 5.46 ± 2.41 °C) and 2015
193 (mean SST 6.13 ± 2.18 °C) had similar warm SSTs towards the central and southwest portion of
194 the survey, and colder SSTs across the northeast portion; however, 2012 was colder in the
195 northeast region (Fig. 2). Sea surface temperatures in 2014 (mean SST 3.09 ± 1.62 °C) were
196 colder over the entire survey area and had substantially less northeast to southwest variability.
197 Randall et al. (2019) using the mean bottom temperatures in the central region, found 2013 (-
198 1.4 °C) to be the coldest year, with 2011-2012 and 2014-2015 having similar warmer bottom
199 temperatures (~ 2 °C). Similarly, differences between years were evident from initial dates at
200 which ice concentration was less than 10% (Table 1). Sea-ice remained in the northeast region
201 until mid to late August in years 2012-2014, and melted in mid- to late July in 2011 and 2015.

202 Monthly mean northward transport (Sv) through the Bering Strait tended to peak in the
203 spring and summer (\sim May-August), with lower transport in the winter (Fig. 3). Higher
204 spring/summer transport occurred in 2011 and 2015, peaking at around $1.92 (\pm 0.09)$ Sv in May

205 and 1.87 (± 0.06) Sv in July of 2015 and 1.91 (± 0.10) Sv in June of 2011. Spring and summer
206 transport was moderate in 2014 and lower in 2012 and 2013, with mean values as low as 1.14 (\pm
207 0.18) and 1.18 (± 0.14) in August of 2012 and 2013, respectively.

208

209 3.2. Zooplankton abundance

210

211 Average pelagic amphipod abundances increased from 2011 to 2015; average benthic
212 abundances were generally higher than pelagic abundances but also increased over the same
213 period (Fig. 4a). Overall, 2013 and 2011 had the highest and lowest average amphipod
214 abundance respectively. Mysid epibenthic and pelagic abundances were relatively low across all
215 years (Fig. 4b), but epibenthic abundances were relatively higher in all years and there were no
216 increasing or decreasing trends across the years. The euphausiids community consisted of four
217 species of the genus *Thysanoessa*: *T. inermis*, *T. longipes*, *T. spinifera*, and *T. raschii*; the latter,
218 being the most abundant (approximately 70% of total abundance) of the four, was singled out in
219 this study for purposes of simplicity. Epibenthic *T. raschii* abundances were lowest in 2013 and
220 highest in 2014 (Fig. 4c). Pelagic *T. raschii* abundance was lowest in 2011 and highest in 2015.

221 There were no consistent differences in the abundance of *T. raschii*, mysid, and
222 amphipods between the bottom layer and water column when we took into account year and a
223 depth-year interaction in our analyses. ANOVA results did not show significant differences
224 between epibenthic and pelagic *T. raschii* abundances independent of year. However, *T. raschii*
225 abundance did show significant differences between years ($F = 3.20$, $p = 0.01$), independent of
226 depth and depth/year interactions ($F = 5.56$, $p < 0.001$). Similarly, ANOVA results did not show
227 significant differences between epibenthic and pelagic amphipods independent of year ($F = 2.16$,

228 $p = 0.14$). However, amphipod abundances did show significant differences among years
229 independent of depth ($F = 4.467$, $p = 0.001$) and depth/year interactions ($F = 3.294$, $p = 0.01$).
230 ANOVA results showed significant differences between epibenthic and pelagic mysids
231 independent of year ($F = 9.59$, $p = 0.002$), years independent of depth ($F = 4.80$, $p = 0.0008$), and
232 depth/year interactions ($F = 0.84$, $p = 0.50$). Time of day was hypothesized to influence
233 euphausiid abundance, however, ANOVA results did not find differences in day/night sampling
234 abundances of *T. raschii* at the $p < 0.05$ significance level.

235 A post-hoc Tukey's 'Honest Significant Difference' test of depth-year interactions of *T.*
236 *raschii*, mysids, and amphipods showed 2014 and 2015 were significantly ($p < 0.05$) different
237 from most previous years (Table 3). Within years 2014 and 2015, *T. raschii* showed significant
238 ($p < 0.05$) differences between epibenthic and pelagic depths. Similarly, both mysids and
239 amphipods showed significant ($p < 0.05$) differences between epibenthic and pelagic depths
240 within 2014. Overall, we cannot independently assess year without noting whether *T. raschii*,
241 mysids, or amphipods samples were caught in the water column or just above the bottom.

242 There was a lack of spatial differences among years for amphipods, with positive catches
243 across all regions (Fig. 5a). The highest amphipod frequency of occurrence was in 2013, with
244 complete absence in only one station (epibenthic and pelagic combined). Mysid abundance was
245 low for each year across all regions (Fig. 5b); within years, more mysids were captured in the
246 northeast than other regions. Mysid had the highest frequency of occurrence in 2014 with
247 animals captured at stations in 3 of the 4 regions (epibenthic and pelagic combined). A lack of
248 spatial differences of *T. raschii* among years was evident (Fig. 5c), with positive catches
249 appearing across most regions. The highest *T. raschii* frequency of occurrence was in 2014, with
250 presence detected from at least one station in three of the four areas (epibenthic and pelagic

251 combined). There were no obvious trends in presence/absence or abundance as a function of
252 distance from land.

253 Abundances of *C. glacialis* were lower in warmer years (2011, 2014, and 2015) and
254 higher in colder years (2012, 2013; Fig. 6). *Calanus glacialis* were ubiquitous across all regions,
255 with presence detected at most stations (Fig. 7).

256

257 3.3. Early life stages

258

259 Development time calculations suggest that it takes approximately 51 and 78 days at 8
260 and 2°C water temperature, respectively, for *Thysanoessa* spp. stages to develop from eggs to
261 furcilia (Table 2). Note that the furcilia counted in this study were not identified to species.
262 Euphausiid furcilia stages were most abundant in the central and southwestern regions of each
263 year (Fig. 8). Euphausiid furcilia were completely absent from the northeastern region in 2012
264 and 2013. Both 2011 and 2014 had similar abundances along the central and southeastern
265 regions, with 2011 having slightly higher abundances in the northeast. In 2015, highest
266 abundances were located in the central region, with lower abundances extending into the
267 northeast. Euphausiid calytopis, a developmental stage of much shorter duration (~40 days
268 shorter; Tegllus et al., 2015), were only caught in very low abundances ($\sim 1.0 \log_{10} (\text{Num. m}^{-2})$)
269 in 2011 at 3 stations (map not shown) from the northeast and southwest regions.

270 Spear et al. (2019) estimated *C. glacialis* egg to C2 stages have approximate development
271 times of 8 to 12 days at temperatures ranging between 12 and -1.5 °C respectively. *Calanus*
272 *glacialis* C2 stages were almost exclusively caught in the northeast region, including Icy Cape

273 (Fig. 9). Higher total abundances appeared in both 2012 ($4.92 \log_{10} (\text{Num. m}^{-2})$) and 2013 (5.19
274 $\log_{10} (\text{Num. m}^{-2})$), while the lowest total abundances were in 2011 ($3.38 \log_{10} (\text{Num. m}^{-2})$).

275

276 3.4. Relationships between plankton abundance and physical variables

277

278 Bottom temperature, 30-day northeastward transport, longitude, and ordinal day were the
279 most significant variables associated with mean *T. raschii* abundance (Table 4). The model
280 helped explain 42.3% of the deviance with an r^2 of 0.38. Extreme lower and higher bottom
281 temperature conditions were associated with lower *T. raschii* abundance (Fig. 10). There was a
282 positive relationship between 30-day northeastward transport and *T. raschii* abundance. The
283 longitude parameter also showed that *T. raschii* abundance was positively associated with the
284 northeastern and southwestern portions of the study area. The strong positive relationship with
285 ordinal day showed that higher abundances showed up later in the year in 2014. This is because
286 the only year in which we sampled past day of year 260 was 2014. Furcilia abundance had
287 significant relationships with bottom temperature, 14-day northeastward transport, year, ordinal
288 day, and longitude. The model explained 56.8% deviance in abundance for euphausiid furcilia
289 with an r^2 of 0.53 (Table 4). There was not a clear abundance pattern in relation to the bottom
290 temperature (Fig. 11). In contrast to the relationship between transport and *T. raschii* adults,
291 there was a negative relationship with furcilia abundance and 14-day northeastward transport.

292 The model helped explain 43% of the deviance with an r^2 of 0.39 of the *C. glacialis* C5
293 stage (Table 4). The most significant parameters included surface salinity, surface temperature,
294 bottom temperature, 14-day transport, ordinal day, and year. Higher surface temperatures had a
295 positive association, while lower surface had a slightly negative association, with C5 abundances

296 (Fig. 12). Conversely, lower bottom temperatures had a positive relationship and higher bottom
297 temperatures had a negative relationship with C5 abundance. Stage C5 abundance was also
298 negatively associated with lower salinity seawater. There was a slight negative association with
299 strong northeastward transport and C5 abundance. Interestingly, there was not a significant
300 association with northeastward transport and *C. glacialis* C2 stages. The C2 stage was similar to
301 C5 stages in the relationship with bottom temperatures, as there was a negative relationship with
302 higher bottom temperatures and a positive relationship lower bottom temperatures (Fig. 13).
303 There was positive association of C2 stages with higher longitudes. Overall, C2 stages had the
304 strongest GAM model, which explained 57% of the deviance and a r^2 of 0.55 (Table 4).

305

306

307 **4. Discussion**

308

309 *4.1. Euphausiid transport*

310

311 *T. raschii* is an amphiboreal species whose distribution also extends to the Arctic Ocean
312 and associated continental shelves. We observed the presence of *T. raschii* in all years near
313 Utqiagvik, with relatively high abundances in 2014 and 2015. The annual presence of
314 euphausiids there is important as they are a dominant component of the diet for bowhead whales
315 in the region (Lowry et al., 2004; Moore et al., 2010). A positive association with northeastward
316 transport and a positive association with higher longitudes, implies that *T. raschii* were advected
317 from the south. The positive association with lower longitudes may be the result of krill being
318 advected into the Chukchi Shelf from the Beaufort Sea as described by Ashjian et al., (2010);

319 other explanations include lack of sampling in the central region in 2013, sampling later in the
320 2014, or because of the current patterns that tend to extend farther offshore in the central region
321 (Stabeno et al., 2018), resulting in animal presence just outside of the sampled transect. Overall,
322 these findings support the hypothesis of Berline et al. (2008) and Ashjian et al. (2010) that the
323 euphausiids concentrated by physical processes near Barrow Canyon likely originated from the
324 northern Bering Sea.

325 Conversely, temperature-dependent euphausiid furcilia development times suggest their
326 extent into the central and northeast regions in warmer conditions was a result of spawning in the
327 Chukchi Sea. Transport of water takes ~90 days to reach Icy Cape from the Bering Strait
328 (Stabeno et al., 2018). This is roughly 12 to 40 days longer than the development time from egg
329 to furcilia at comparable temperatures. The hypothesis of local production is also supported by
330 the negative relationship with 14-day transport or lack of clear relationship with bottom
331 temperatures. In particular, the negative relationship with 14-day transport (in addition to a lack
332 of association with 30-day transport) showed that the greater and more recent transport resulted
333 in reduced abundances, suggesting they were likely recently spawned nearby and subsequently
334 transported away.

335 Adult euphausiids were present in the northeast region in 2012 and 2013, even though
336 overall transport during those years was low. The absence of younger stages could have resulted
337 from a change in the timing of reproduction relative to our sampling, failed spawning, or very
338 high mortality of the larvae because of cold temperatures or high predation. Euphausiid eggs
339 were present in the northeast region in 2014 and 2015, but were absent in 2012 and 2013 (egg
340 data not collected in 2011), suggesting reproduction only occurred when this region was not
341 occupied by colder water masses.

342 The higher pelagic abundances of euphausiids in 2013 and 2015 were not due to a
343 day/night effect as a comparison of day/night abundances found no significant differences (not
344 shown). The significant increase in abundance of *T. raschii* in 2014, compared to remaining
345 years, suggests that sampling later in the season likely had considerable impact. This is
346 evidenced by the relationship between ordinal day and euphausiid abundance in 2014. Other
347 environmental and physical results did not suggest any other anomalous features that may have
348 caused this significant jump in abundance. Thus, it suggests that because we sampled later in
349 2014 we observed more euphausiids compared to other years. This is most likely the result of
350 advection timing (as explained in Berline et al., 2008), but may also reflect local recruitment.
351 Alternative explanations for increased abundance include local production or retained for a
352 longer period of time. Most historical surveys have not sampled later than mid-September to
353 avoid disturbing subsistence hunting by Iñupiat whalers as the whales migrate westward from the
354 Beaufort. Thus previous surveys (Grebmeier and Harvey, 2005; Lane et al., 2008) reporting low
355 numbers of euphausiids could be due to the mismatch between euphausiid transport from the
356 south and survey timing.

357 Our estimates of adult euphausiid abundance may be somewhat improved over prior
358 estimates derived from small mouth plankton nets towed only in the water column (e.g. Eisner et
359 al., 2013). However, euphausiids are difficult to accurately estimate even with larger nets that
360 sample at faster tow speeds. (e.g. Hunt et al., 2016). Net avoidance by euphausiids has long been
361 recognized as chronic problem in oceanographic studies (e.g. Brinton, 1967; Herman et al., 1993;
362 Sameoto et al., 2011; Wiebe et al., 2013). Net avoidance abilities may even extend to the young
363 stages (e.g. Smith, 1991). Future work using acoustical or optical techniques may be able to

364 provide better estimates of euphausiid abundance, although as this study demonstrated there is a
365 need to sample very close to the seafloor.

366

367 4.2. Other large zooplankton

368

369 We found that *C. glacialis* were most abundant in colder conditions, with the abundance
370 increase being driven by earlier development stages. This finding is supported by research
371 showing that *C. glacialis* were strongly tied to the ice edge algae production, which is increased
372 in colder years (Søreide et al., 2010). Both C2 and C5 stages showed a significant positive
373 association with colder bottom temperatures. The C5 stage, as opposed to the C2 stage, also had
374 a positive association with warmer surface temperatures and significant relationship with
375 northeastward transport, suggesting that C5 stages were more likely to be influenced by
376 advection. The C2 stage had significantly higher abundances in the northeast region, a negative
377 relationship with higher surface temperatures, and lack of a significant relationship with
378 transport, suggesting local production rather than transported from the south. This is supported
379 by previous research showing *C. glacialis* having approximate development times of 8 to 12
380 days at temperatures between 12 and -1.5°C, respectively, from egg to C2 stage (Hirst and
381 Lampitt, 1998; Kiørboe and Hirst, 2008; Spear et al., 2019). As described earlier, transport times
382 from the Bering Sea to the northeast region were much longer than development times from egg
383 to C2 Stage. C2 copepodites were also more abundant in 2012 and 2013, when temperatures
384 were coldest in the northeast. This suggests that the overall abundance increases in *C. glacialis* in
385 2012 and 2013, when temperatures were colder, sea ice melted later in the northeast region, and
386 advection was lower, was primarily due to local reproduction. Abundance increases in the

387 northeast region could also be due to upwelling onto the Chukchi Shelf from the Beaufort Sea
388 (Ashjian et al., 2010). Conversely, the lower abundances of C2 stages in warmer conditions may
389 be a result of faster and earlier development into later stages. Thus the various stages of *C.*
390 *glacialis* region likely have multiple sources (in situ reproduction and transport from the south
391 and east), and the absolute abundance is a function of local and regional processes. This is a
392 notable result; later stages of *C. glacialis* are known to be the primary prey of bowhead whales
393 around West Greenland (Heide-Jørgensen et al., 2013), and a significant contribution to their diet
394 in the Chukchi and Beaufort seas (Lowry et al., 2004; Moore et al., 2010). In addition, if *C.*
395 *glacialis* are developing faster, they may enter into diapause earlier creating a mismatch with
396 migrating whales.

397 The significant differences in pelagic and epibenthic abundance in both mysids and
398 amphipod highlights the importance of sampling near the bottom. Mysids and some amphipod
399 species may spend time in the water column; therefore, sampling the water column and
400 epibenthic layer will yield improved estimates of their abundance. Epibenthic amphipod
401 abundance was significantly higher in 2013 than any other year sampled in this study. This is a
402 notable observation in the context of a changing climate, given that 2013 was also the coldest
403 year and certain species of amphipods, in particular, have known ice-associated and bottom
404 dwelling habits (Vinogradov, 1999; Gradinger and Bluhm, 2004). Both amphipods and mysids
405 are prey for multiple marine mammals, including bearded seals (*Erignathus barbatus*; Cameron
406 et al., 2010), Pacific walrus (*Odobenus rosmarus divergens*; Sheffield and Grebmeier, 2009),
407 beluga whales (*Delphinapterus leucas*; Quakenbush et al., 2015), gray whales (*Eschrichtius*
408 *robustus*; Nerini, 1984; Darling et al., 1998), and bowhead whales (Lowry et al., 2004). Given

409 the importance of mysids and amphipods to Arctic food webs, it is important to monitor their
410 response to changes in ice cover and water temperatures.

411

412 4.3. Chukchi Sea large zooplankton status and trends

413

414 The findings of this study are relevant to the potential response of lower trophic levels to
415 climate warming, including changes in Arctic food webs. Recent studies have found a 50%
416 increase in water volume transport through the Bering Strait to the Chukchi Sea from 2001-2014;
417 the immediate impact to the physical environment is an increase in heat flux that is a potential
418 trigger for Arctic sea-ice melt and retreat (Woodgate et al., 2010, 2015; Woodgate, 2018). As
419 the climate warms, increases in primary and secondary production will result in changes in
420 abundance of lipid-rich zooplankton, but it remains to be seen what the overall lipid availability
421 will be (Renaud et al., 2018). Two of the species targeted in this study, *C. glacialis* and *T.*
422 *raschii*, have an average percent lipid content of approximately 11-15% and 3-5%, respectively,
423 both having a higher average percent lipid content in colder years (Heintz et al., 2013). There is a
424 general consensus that densities of sea ice-associated, lipid-rich *C. glacialis* are expected to
425 decline due to loss of ice in the region. (Tremblay et al., 2012; Arrigo and Van Dijken, 2015;
426 Grebmeier et al., 2006a; Grebmeier, 2012; Moore and Stabeno, 2015; Renaud et al., 2018). In
427 addition, this study provides evidence that increases in large zooplankton abundance such as
428 euphausiids (which also contain depot lipids) is likely to occur, either via advection from lower
429 latitudes or changes in local production. This is supported by previous studies which found an
430 increase in zooplankton biomass over several decades in the Chukchi Sea (Ershova et al., 2015).
431 An increase in abundance of prey such as euphausiids will likely benefit higher trophic level

432 predators such as planktivorous fish, seabirds and marine mammals. Recently, studies have
433 suggested that the abundance of other planktivores in the northern Bering Sea and Chukchi
434 appear to be changing. For example, in the Bering Sea, there has been a decrease in the lipid-
435 rich nodal species Arctic cod (*Boreogadus saida*) and an increase in the commercial species
436 walleye pollock (*Gadus chalcogrammus*) and Pacific cod (*Gadus macrocephalus*; Stevenson and
437 Lauth, 2019). Walleye pollock have been observed in the Chukchi and Beaufort seas (e.g.
438 Logerwell et al., 2015) and is an important planktivore in the southeastern Bering Sea ecosystem
439 consuming both euphausiids and large copepods (Dwyer et al., 1987;
440 <https://access.afsc.noaa.gov/REEM/WebDietData/DietDataIntro.php>). Walleye pollock could
441 become an effective competitor for large zooplankton with other fishes, seabirds, and marine
442 mammals if its abundance continues to increase in the northern Bering, Chukchi and Beaufort
443 seas. At present, however, there is evidence of improved body condition of bowhead whales
444 returning from the Beaufort (George et al., 2015). This suggests that the plankton community in
445 their summer feeding grounds has changed in either biomass, species composition or both.

446 The strong interaction between top-predators (whales, seabirds, and Arctic cod) and
447 copepods/krill in the northern Chukchi appeared to be mediated by both advection and local
448 production related to sea-ice dynamics. What remains to be seen is whether arctic shelf
449 ecosystems will continue to be bottom-up forced by sea-ice dynamics or whether climate-
450 mediated impacts on intermediate trophic levels (e.g. large zooplankton and small fishes) could
451 become the predominant controlling mechanism, e.g. wasp-waist control (Gaichas et al., 2015;
452 Griffiths et al., 2013; Fauchald et al., 2011). If warming continues, the bottom-up dynamics in
453 this location would likely be disrupted by increased advection over longer time-periods as well

454 as a lack of localized, lipid-rich, ice-associated production. Such a shift would greatly impact the
455 trophic dynamics in the region.

456

457

458 **5. Conclusions**

459

460 This study analyzed five successive years of zooplankton abundance over a wide range of
461 physical oceanographic characteristics in the Chukchi Sea to better understand the status and
462 trends in prey availability for baleen whales, seabirds, and planktivorous fish. The coldest year
463 (2013) was highlighted by later summer sea-ice melt, colder sea surface and bottom
464 temperatures, and lower northward transport through the Bering Strait during the spring and
465 summer months. Generally, the warmest years accompanied with earlier summer sea-ice melt,
466 warmer sea surface and bottom temperatures, and higher Bering Strait transport during the spring
467 and summer months. Adult euphausiid abundances differed across warm and cold conditions.
468 These differences appeared most pronounced regionally (NE-SW gradient) and were related to
469 transport, which suggests that most of these euphausiids are transported to the Chukchi Sea from
470 the Bering Sea. The lack of furcilia in 2012 and 2013, (except in the SW), and the presence of
471 furcilia in 2011 and 2014-15, suggests that only in these warmer years with higher advection
472 were earlier stages transported to the northeast region of the Chukchi Sea. We also found that
473 some euphausiids might be locally produced based on the development times. In contrast, the *C.*
474 *glacialis* C5 stages were found across all years, but C2 stages were found primarily in the
475 northeast and were more abundant under colder conditions which suggests local production of
476 copepods. Thus, the large numbers of euphausiids and copepods that dominate the prey in

477 stomachs of bowhead whales harvested near Utqiagvik, Alaska (Lowry et al., 2004; Ashjian et
478 al., 2010; Moore et al., 2010; George et al., 2015) are likely the result of transport of euphausiids
479 to this location and the contribution of locally produced *C. glacialis*, although *Calanus* found in
480 the region potentially come from several sources or origins.

481

482

483 **Acknowledgements**

484

485 The authors would like to thank Captain Fred Roman, F/V *Mystery Bay*, Captain Kale
486 Garcia, R/V *Aquila*, and Captain/C.O. Robert A. Kamphaus, NOAA ship *Ronald H. Brown*, as
487 well as all crew members. Special thanks also go to Catherine Berchok and Nanci Kachel for
488 their leadership; Bill Floering and David Strausz for assistance at sea, Rebecca Woodgate for
489 suggestions and sharing physical data; the Bering Strait mooring project; Polish Plankton Sorting
490 and Identification Center for processing and enumerating zooplankton samples; and North
491 Pacific Climate Regimes and Ecosystem Productivity (NPCREP) program for support. This
492 research was part of the Chukchi Sea Acoustics, Oceanography and Zooplankton Extension
493 (CHAOZ-X) and Arctic Whale Ecology Study (ArcWEST) which were funded by the Bureau of
494 Ocean Energy Management (BOEM; Contract No. M13PG00026 and M12PG00021). Reference
495 to trade names does not imply endorsement by the National Marine Fisheries Service, NOAA.

496

497

498 **References**

- 499 Ashjian, C.J., Braund, S.R., Campbell, R.G., Gearge, J.C., Kruse, J., Maslowski, W., Moore,
500 S.E., Nicolson, C.R., Okkonen, S.R., Sherr, B.F., 2010. Climate variability, oceanography,
501 bowhead whale distribution, and Iñupiat subsistence whaling near Barrow, Alaska. *Arctic*,
502 179-194. <https://doi.org/10.14430/arctic973>
- 503 Ashjian, C.J., Campbell, R.G., Gelfman, C., Alatalo, P., Elliott, S.M., 2017. Mesozooplankton
504 abundance and distribution in association with hydrography on Hanna Shoal, NE Chukchi
505 Sea, during August 2012 and 2013. *Deep-Sea Res. II* 144, 21-36.
506 <https://doi.org/10.1016/j.dsr2.2017.08.012>
- 507 Berline, L., Spitz, Y.H., Ashjian, C.J., Campbell, R.G., Maslowski, W., Moore, S.E., 2008.
508 Euphausiid transport in the western Arctic Ocean. *Mar. Ecol. Prog. Ser.* 360, 163-178.
509 <https://doi.org/10.3354/meps07387>
- 510 Bond, N., Stabeno, P., Napp, J., 2018. Flow patterns in the Chukchi Sea based on an Oceano
511 Reanalysis, June through October 1979 – 2014. *Deep-Sea Res. II* 152, 35-47.
512 <https://doi.org/10.1016/j.dsr2.2018.02.009>
- 513 Brinton, E., 1967. Vertical migration and avoidance capability of euphausiids in the California
514 Current. *Limnol. Oceanogr.* 12, 451-483. <https://doi.org/10.4319/lo.1967.12.3.0451>
- 515 Cameron, M.F., Bengtson, J.L., Boveng, P.L., Jansen, J.K., Kelly, B.P., Dahle, S.P., Logerwell,
516 E.A., Overland, J.E., Sabine, C.L., Waring, G.T., Wilder, J.M., 2010. Status review of the
517 bearded seal (*Erignathus barbatus*). U.S. Dep. Commer, NOAA Tech Memo NMFS-
518 AFSC-211, 246

519 Campbell, R.G., Sherr, E.B., Ashjian, C.J., Plourde, S., Sherr, B.F., Hill, V., Stockwell, D.A.,
520 2009. Mesozooplankton prey preference and grazing impact in the western Arctic Ocean.
521 Deep-Sea Res. II 56, 1274-1289. <https://doi.org/10.1016/j.dsr2.2008.10.027>

522 Citta, J.J., Quakenbush, L.T., George, J.C., Small, R.J., Heide-Jorgensen, M.P., Brower, H.,
523 Adams, B., Brower, L., 2012. Winter movements of bowhead whales (*Balaena mysticetus*)
524 in the Bering Sea. Arctic 65, 13–34. <https://doi.org/10.14430/arctic4162>

525 Comiso, J., 1999. Bootstrap sea ice concentrations for NIMBUS-7 SMMR and DMSP SSM/I.
526 Digital Media, National Snow and Ice Data Center 10.

527 Coyle, K., Pinchuk, A., 2002. Climate-related differences in zooplankton density and growth on
528 the inner shelf of the southeastern Bering Sea. Prog. Oceanogr. 55, 177-194.
529 [https://doi.org/10.1016/S0079-6611\(02\)00077-0](https://doi.org/10.1016/S0079-6611(02)00077-0)

530 Danielson, S.L., Eisner, L., Ladd, C., Mordy, C., Sousa, L., Weingartner, T.J., 2017. A
531 comparison between late summer 2012 and 2013 water masses, macronutrients, and
532 phytoplankton standing crops in the northern Bering and Chukchi Seas. Deep-Sea Res. II
533 135, 7-26. <https://doi.org/10.1016/j.dsr2.2016.05.024>

534 Darling, J.D., Keogh, K.E., Steeves, T.E., 1998. Gray whale (*Eschrichtius robustus*) habitat
535 utilization and prey species off Vancouver Island, BC. Mar. Mammal Sci. 14, 692-720.
536 <https://doi.org/10.1111/j.1748-7692.1998.tb00757.x>

537 Dwyer, D.A., Bailey, K.M., Livingston, P.A., 1987. Feeding habits and daily ration of walleye
538 pollock (*Theragra chalcogramma*) in the eastern Bering Sea with special reference to
539 cannibalism. Can. J. Fish Aquat. Sci. 44, 1972-1984. <https://doi.org/10.1139/f87-242>

540 Eisner, L., Hillgruber, N., Martinson, E., Maselko, J., 2013. Pelagic fish and zooplankton species
541 assemblages in relation to water mass characteristics in the northern Bering and southeast
542 Chukchi seas. *Polar Biol.* 36, 87-113. <https://doi.org/10.1007/s00300-012-1241-0>

543 Ershova, E.A., Hopcroft, R.R., Kosobokova, K.N., Matsuno, K., Nelson, R.J., Yamaguchi, A.,
544 Eisner, L.B., 2015. Long-term changes in summer zooplankton communities of the western
545 Chukchi Sea, 1945–2012. *Oceanography* 28, 100-115.
546 <https://doi.org/10.5670/oceanog.2015.60>

547 Fauchald, P., Skov H., Skern-Mauritzen, M., Johns, D., Tveraa, T. 2011. Wasp-waist
548 interactions in the North Sea Ecosystem. *PLoS One* 6: e22729,
549 <https://doi.org/10.1371/journal.pone.0022729>

550 Gaichas, S., Aydin K., Francis, R.C., 2015. Wasp waist or beer belly? Modeling food web
551 structure and energetic control in Alaskan marine ecosystems, with implications for fishing
552 and environmental forcing. *Prog. Oceanogr.* 138, 1-17.
553 <https://doi.org/10.1016/j.pocean.2015.09.010>

554 George, J.C., Druckenmiller, M.L., Laidre, K.L., Suydam, R., Person, B., 2015. Bowhead whale
555 body condition and links to summer sea ice and upwelling in the Beaufort Sea. *Prog.*
556 *Oceanogr.* 136, 250-262. <https://doi.org/10.1016/j.pocean.2015.05.001>

557 Gong, D., Pickart, R.S., 2015. Summertime circulation in the eastern Chukchi Sea. *Deep-Sea*
558 *Res. II.* 118, 18-31. <https://doi.org/10.1016/j.dsr2.2015.02.006>

559 Gradinger, R.R., Bluhm, B.A., 2004. In-situ observations on the distribution and behavior of
560 amphipods and Arctic cod (*Boreogadus saida*) under the sea ice of the High Arctic Canada
561 Basin. *Polar Biol.* 27, 595-603. <https://doi.org/10.1007/s00300-004-0630-4>

562 Grebmeier, J. M., Harvey, H.R., 2005. The Western Arctic Shelf? Basin Interactions (SBI)
563 project: An overview. Deep-Sea Res. II. 52, 3109-3115.
564 <https://doi.org/10.1016/j.dsr2.2005.10.004>

565 Grebmeier, J.M., Cooper, L.W., Feder, H.M., Sirenko, B.I., 2006a. Ecosystem dynamics of the
566 Pacific-influenced northern Bering and Chukchi seas in the Amerasian Arctic. Prog.
567 Oceanogr. 71, 331-361. <https://doi.org/10.1016/j.pocean.2006.10.001>

568 Grebmeier, J.M., Overland, J.E., Moore, S.E., Farley, E.V., Carmack, E.C., Cooper, L.W., Frey,
569 K.E., Helle, J.H., McLaughlin, F.A., McNutt, S.L., 2006b. A major ecosystem shift in the
570 northern Bering Sea. Science 311, 1461-1464. <https://doi.org/10.1126/science.1121365>

571 Grebmeier, J.M., 2012. Shifting patterns of life in the Pacific Arctic and Sub-arctic Seas. Ann.
572 Rev. Mar. Sci. 4, 63-78. <https://doi.org/10.1146/annurev-marine-120710-100926>

573 Griffiths, S.P., Olson, R.J., Watters, G.M., 2013. Complex wasp-waist regulation of pelagic
574 ecosystems in the Pacific Ocean. Rev. Fish Biol. Fisher. 23, 459-475.
575 <https://doi.org/10.1007/s11160-012-9301-7>

576 Heide-Jørgensen, M.P., Laidre, K.L., Nielsen, N.H., Hanson, R.G., Røstand, A., 2013. Winter
577 and spring diving behavior of bowhead whales relative to prey. Anim. Biotel. 1, 15.
578 <https://doi.org/10.1186/2050-3385-1-15>

579 Heintz, R.A., Siddon, E.C., Farley, E.V., Napp, J.M., 2013. Correlation between recruitment and
580 fall condition of age-0 pollock (*Theragra chalcogramma*) from the eastern Bering Sea
581 under varying climate conditions. Deep-sea Res II 94, 150-156.
582 <https://doi.org/10.1016/j.dsr2.2013.04.006>

583 Hirst, A.G., Lampitt R.S., 1998. Towards a global model of in situ weight-specific growth in
584 marine planktonic copepods. *Mar. Biol.* 132, 247-257.
585 <https://doi.org/10.1007/s002270050390>

586 Hopcroft, R.R., Kosobokova, K.N., Pinchuk, A.I., 2010. Zooplankton community patterns in the
587 Chukchi Sea during summer 2004. *Deep-Sea Res. II* 57, 27-39.
588 <https://doi.org/10.1016/j.dsr2.2009.08.003>

589 Hunt, G.L., Ressler, P.H., Gibson, G.A., De Robertis, A., Aydin, K., Sigler, M.F., Ortiz, J.,
590 Lessard, E.J., Williams, B.C., Pinchuk, A., Buckley, T., 2016. Euphausiids in the eastern
591 Bering Sea: A synthesis of recent studies of euphausiid production, consumption, and
592 population control. *Deep-Sea Res. II* 134, 204-222.
593 <https://doi.org/10.1016/j.dsr2.2015.10.007>

594 Kiørboe, T., Hirst, A. G., 2008. Optimal development time in pelagic copepods. *Mar. Ecol. Prog.*
595 *Ser.* 367, 15-22. <https://doi.org/10.3354/meps07572>

596 Lane, P. V., Llinás, L., Smith, S. L., Pilz, D., 2008. Zooplankton distribution in the western
597 Arctic during summer 2002: hydrographic habitats and implications for food chain
598 dynamics. *J. Mar. Sys.* 70, 97-133. <https://doi.org/10.1016/j.jmarsys.2007.04.001>

599 Logerwell, E., Busby, M., Carothers, C., Cotton, S., Duffy-Anderson, J., Farley, E., Goddard, P.,
600 Heintz, R., Holladay, B., Horne, J., Johnson, S., Lauth, B., Moulton, L., Neff, D., Norcross,
601 B., Parker-Stetter, S., Siegle, J., Sformo, T., 2015. Fish communities across a spectrum of
602 habitats in the western Beaufort Sea and Chukchi Sea. *Prog. Oceanogr.* 136, 115 – 132.
603 <https://doi.org/10.1016/j.pocean.2015.05.013>

604 Lowry, L.F., Sheffield, G., George, J.C., 2004. Bowhead whale feeding in the Alaskan Beaufort
605 Sea, based on stomach contents analyses. *J. Cetacean Res. Manage.* 6, 215-223.

606 Moore, S.E., Stafford, K.M., Munger, L.M., 2010. Acoustic and visual surveys for bowhead
607 whales in the western Beaufort and far northeastern Chukchi seas. *Deep-Sea Res. II* 57,
608 153-157. <https://doi.org/10.1016/j.dsr2.2009.08.013>

609 Moore, S.E., Stabeno, P.J., 2015. Synthesis of Arctic Research (SOAR) in marine ecosystems of
610 the Pacific Arctic. *Prog. Oceanogr.* 136, 1-11.
611 <https://doi.org/10.1016/j.pocean.2015.05.017>

612 Nerini, M., 1984. A review of gray whale feeding ecology. *The gray whale, Eschrichtius*
613 *robustus*, 423-450.

614 Perovich, D.K., Farrell, S., Gerland, S., Hendricks, S., Kaleschke, L., Meier, W., Ricker, R.,
615 Tian-Kunze, X., Tschudi, M., Webster, M., Wood, K., 2019. Sea Ice [in Arctic Report
616 Card 2019]. <http://www.arctic.noaa.gov/reportcard>

617 Pinchuk, A.I., Eisner, L.B., 2017. Spatial heterogeneity in zooplankton summer distribution in
618 the eastern Chukchi Sea in 2012–2013 as a result of large-scale interactions of water
619 masses. *Deep-Sea Res. II* 135, 27-39. <https://doi.org/10.1016/j.dsr2.2016.11.003>

620 Pinchuk, A.I., Hopcroft, R.R., 2006. Egg production and early development of *Thysanoessa*
621 *inermis* and *Euphausia pacifica* (Crustacea: Euphausiacea) in the northern Gulf of Alaska.
622 *J. Exp. Mar. Biol. Ecol.* 332, 206-215. <https://doi.org/10.1016/j.jembe.2005.11.019>

623 Pinchuk, A.I. and Hopcroft, R.R., 2007. Seasonal variations in the growth rates of euphausiids
624 (*Thysanoessa inermis*, *T. spinifera*, and *Euphausia pacifica*) from the northern Gulf of
625 Alaska. *Mar. Biol.* 151, 257-269. <https://doi.org/10.1007/s00227-006-0483-1>

626 Questel, J.M., Clarke, C., Hopcroft, R.R., 2013. Seasonal and interannual variation in the
627 planktonic communities of the northeastern Chukchi Sea during the summer and early fall.
628 *Cont. Shelf Res.* 67, 23-41. <https://doi.org/10.1016/j.csr.2012.11.003>

629 Quakenbush, L.T., Citta, J.J., George, J.C., Small, R.J., Heide-Jørgensen, M.P., 2010. Fall and
630 winter movements of bowhead whales (*Balaena mysticetus*) in the Chukchi Sea and within
631 a potential petroleum development area. *Arctic* 63, 289–307.
632 <https://doi.org/10.14430/arctic1493>

633 Quakenbush, L., Suydam, R.S., Bryan, A.L., Lowry, L.F., Frost, K.J. and Mahoney, B.A., 2015.
634 Diet of beluga whales (*Delphinapterus leucas*) in Alaska from stomach contents, March–
635 November. *Mar. Fish. Rev.* 77, 70-84.

636 R Core Team, 2019. R: A language and environment for statistical computing. R Foundation for
637 Statistical Computing, Vienna, Austria. <https://www.R-project.org/>

638 Randall, R. J., Busby, M.S., Spear, A., Mier, K.L., 2019. Spatial and temporal variation of
639 summer ichthyoplankton assemblage structure in the eastern Chukchi Sea 2010-2015.
640 *Polar Biol.* 42, 1811-1824. <https://doi.org/10.1007/s00300-019-02555-8>

641 Renaud, P.E., Daase, M., Banas, N.S., Gabrielsen, T.M., Søreide, J.E., Varpe, Ø., Cottier, F.,
642 Falk-Petersen, S., Halsband, C., Vogedes, D., Heggland, K., Berge J., 2018. Pelagic food-
643 webs in a changing Arctic: a trait-based perspective suggests a mode of resilience. *ICES J.*
644 *Mar. Sci.* 75, 1871-1881. <https://doi.org/10.1093/icesjms/fsy063>

645 Sameoto, D., Cochrane, N.A., Herman, A., 2011. Convergence of acoustic, optical, and net-
646 catch estimates of euphausiid abundance: use of artificial light to reduce net avoidance.
647 *Can. J. Fish. Aquat. Sci.* 50, 334-346. <https://doi.org/10.1139/f93-039>

648 Sheffield, G., Grebmeier, J.M., 2009. Pacific walrus (*Odobenus rosmarus divergens*): differential
649 prey digestion and diet. *Mar. Mammal Sci.* 25, 761-777. [https://doi.org/10.1111/j.1748-](https://doi.org/10.1111/j.1748-7692.2009.00316.x)
650 [7692.2009.00316.x](https://doi.org/10.1111/j.1748-7692.2009.00316.x)

651 Smith, S.L. 1991. Growth, development and distribution of the euphausiids *Thysanoessa raschii*
652 (M.Sars) and *Thysanoessa inermis* (Kroyer) in the southeastern Bering Sea. Polar Res. 10,
653 461-478. <https://doi.org/10.3402/polar.v10i2.6759>

654 Søreide, J.E., Leu, E., Berge, J., Graeve, M., Falk-Petersen, S., 2010. Timing of blooms, algal
655 food quality and *Calanus glacialis* reproduction and growth in a changing Arctic. Glob.
656 Change Biol. 16, 3154-3163. <https://doi.org/10.1111/j.1365-2486.2010.02175.x>

657 Spear, A., Duffy-Anderson, J., Kimmel, D., Napp, J., Randall, J., Stabeno, P., 2019. Physical and
658 biological drivers of zooplankton communities in the Chukchi Sea. Polar Biol. 42, 1107-
659 1124. <https://doi.org/10.1007/s00300-019-02498-0>

660 Stabeno, P., Kachel, N., Ladd, C., Woodgate, R., 2018. Flow patterns in the eastern Chukchi Sea:
661 2010–2015. J. Geophys. Res.-Oceans 123, 1177-1195.
662 <https://doi.org/10.1002/2017JC013135>

663 Stevenson, D.E., Lauth R.R., 2019. Bottom trawl surveys in the northern Bering Sea indicate
664 recent shifts in the distribution of marine species. Polar Biol. 42, 407-421. [https://doi.org/](https://doi.org/10.1007/s00300-018-2431-1)
665 [10.1007/s00300-018-2431-1](https://doi.org/10.1007/s00300-018-2431-1)

666 Tegllhus, F.W., Agersted, M.D., Akther, H., Nielsen, T.G., 2015. Distributions and seasonal
667 abundances of krill eggs and larvae in the sub-Arctic Godthåbsfjord, SW Greenland. Mar.
668 Ecol. Prog. Ser. 539, 111-125. <https://doi.org/10.3354/meps11486>

669 Timmermans, M.-L., Ladd, C., Sea Surface Temperature [in Arctic Report Card 2019].
670 <http://www.arctic.noaa.gov/reportcard>

671 Tremblay, J-É., Robert, D., Varela, D.E., Lovejoy, C., Darnis G., Nelson R.J., Sastri A.R., 2012.
672 Current state and trends in Canadian Arctic marine ecosystems: I. Primary production.
673 Clim. Change 115, 161-178. doi:10.1007/s10584-012-0496-3

674 Vinogradov, G. M., 1999. Deep-sea near-bottom swarms of pelagic amphipods *Themisto*:
675 observations from submersibles. *Sarsia*, 84, 465-467.
676 <https://doi.org/10.1080/00364827.1999.10807352>

677 Wiebe, P.H., Lawson, G.L., Lavery, A.C., Copley, N. J., Horgan, E., Bradley, A., 2013.
678 Improved agreement of net and acoustical methods for surveying euphausiids by mitigating
679 avoidance using a net-based LED strobe light system. *ICES J. Mar. Sci.* 70, 650-664.
680 <https://doi.org/10.1093/icesjms/fst005>

681 Wood, S.N., 2011. Fast stable restricted maximum likelihood and marginal likelihood estimation
682 of semiparametric generalized linear models. *J. Royal Stat. Soc. Ser. B* 73, 3-36.

683 Woodgate, R.A., Aagaard, K., Weingartner, T.J., 2005. A year in the physical oceanography of
684 the Chukchi Sea: Moored measurements from autumn 1990–1991. *Deep-Sea Res. II* 52,
685 3116-3149. <https://doi.org/10.1016/j.dsr2.2005.10.016>

686 Woodgate, R.A., Stafford, K.M., Prahl, F.G., 2015. A synthesis of year-round interdisciplinary
687 mooring measurements in the Bering Strait (1990–2014) and the RUSALCA years (2004–
688 2011). *Oceanography*. 28, 46-67. <https://doi.org/10.5670/oceanog.2015.57>

689 Woodgate, R.A., 2018. Increases in the Pacific inflow to the Arctic from 1990 to 2015, and
690 insights into seasonal trends and driving mechanisms from year-round Bering Strait
691 mooring data. *Prog. Oceanogr.* 160, 124-154.
692 <https://doi.org/doi:10.1016/j.pocean.2017.12.007>

693

694

695

696 **Figure Captions**

697 Fig. 1. Study area in the Chukchi Sea. Each region is symbolized by a colored circle. The study
698 area was split up into southwest, central, northeast, and Beaufort regions. The pink shaded region
699 indicates Barrow Canyon.

700

701 Fig. 2. Sea surface temperature (°C) averaged from 5-10 m for each year.

702

703 Fig. 3. Mean transport (Sv) of water by month for each year through the Bering Strait. The grey
704 underlay highlights the approximate peak transport months.

705

706 Fig. 4. Yearly epibenthic and pelagic total abundance ($\text{Log}_{10}(\text{Num m}^{-2})$) for amphipods (a),
707 mysids (b), and *Thysanoessa raschii* (c).

708

709 Fig. 5. Yearly maps of epibenthic and pelagic total abundance ($\text{Log}_{10}(\text{Num m}^{-2})$) for amphipods
710 (a), mysids (b), and *Thysanoessa raschii* (c). The letter “X” denotes tows where the taxon was
711 absent. Note that the scale differs among taxa.

712

713 Fig. 6. Yearly pelagic total abundance ($\text{Log}_{10}(\text{Num m}^{-2})$) of *Calanus glacialis*.

714

715 Fig. 7. Yearly maps of pelagic total abundance ($\text{Log}_{10}(\text{Num m}^{-2})$) of *Calanus glacialis*. The letter
716 “X” denotes tows where the taxon was absent.

717

718 Fig. 8. Yearly maps of pelagic total abundance ($\text{Log}_{10}(\text{Num m}^{-2})$) of euphausiid furcilia. The
719 letter “X” denotes tows where the taxon was absent.

720

721 Fig. 9. Yearly maps of pelagic total abundance ($\text{Log}_{10}(\text{Num m}^{-2})$) of *Calanus glacialis* C2 stage.

722 The letter “X” denotes tows where the taxon was absent.

723

724 Fig. 10. GAM smooth for the distribution of *Thysanoessa raschii* epibenthic abundance

725 ($\text{Log}_{10}(\text{Num m}^{-2})$), 2011-2015. Variables included mean bottom temperature (a), 30-day

726 transport (b), longitude (c), and day of year (ordinal day) (d).

727

728 Fig. 11. GAM smooth for the distribution of euphausiid furcilia pelagic abundance ($\text{Log}_{10}(\text{Num}$

729 $\text{m}^{-2})$, 2011-2015. Variables included mean bottom temperature (a), 14- day transport (b),

730 longitude (c), day of year (ordinal day) (d), and year (e).

731

732 Fig. 12. GAM smooth for the distribution of *Calanus glacialis* C5 stage pelagic abundance

733 ($\text{Log}_{10}(\text{Num m}^{-2})$), 2011-2015. Variables included mean surface temperature (a), surface bottom

734 salinity (b), bottom temperature (c), 14-day transport (d), day of year (ordinal day) (e), and year

735 (f).

736

737 Fig. 13. GAM smooth for the distribution of *Calanus glacialis* C2 stage pelagic abundance

738 ($\text{Log}_{10}(\text{Num m}^{-2})$), 2011-2015. Variables included mean surface temperature (a), bottom

739 temperature (b), longitude (c), day of year (ordinal day) (d), and year (e).

740

741

742

743

744 **Tables**

745 Table 1. Estimate of the initial date at which ice concentration was less than 10% within the
746 southwest and northeast region of the sampling area.

747

	Southwest	Northeast
748 2011	3 June	15 July
2012	22 June	19 August
749 2013	29 June	31 August
2014	16 June	16 August
750 2015	14 June	18 July

751

752

753

754

755

756

757

758 Table 2. Amount of days at different temperatures for *Thysanoessa* spp. stages to develop from
759 eggs.

Stage	12 °C	8 °C	2 °C	-1.5 °C
760 Calyptopis	13.4	17.8	27.3	35
761 Furcilia	38.2	50.9	78	100

762

763

764

765

766

767

768
769
770
771
772
773
774
775
776
777
778
779
780
781
782
783
784
785
786
787
788
789
790
791
792

Table 3. Post-hoc Tukey's test significant *p* values for the depth-year interactions of each taxon.

	Depth:Year	<i>p</i> value
<i>T. RASCHII</i>	Epibenthic:2014 – Pelagic:2011	0.0200
	Pelagic:2015 – Pelagic:2011	0.0252
	Epibenthic:2014 – Epibenthic:2011	0.0462
	Epibenthic:2014 – Pelagic:2012	0.0179
	Pelagic:2015 – Pelagic:2012	0.0234
	Epibenthic:2014 – Epibenthic:2012	0.0417
	Pelagic:2015 – Epibenthic:2011	0.0494
	Epibenthic:2014 – Pelagic:2014	0.0235
	Pelagic:2015 – Pelagic:2014	0.0307
	Epibenthic:2015 – Epibenthic:2014	0.0342
Epibenthic:2015 – Pelagic:2015	0.0390	
<i>MYSIDS</i>	Epibenthic:2014 – Pelagic:2011	0.0000
	Epibenthic:2014 – Epibenthic:2011	0.0001
	Epibenthic:2014 – Pelagic:2012	0.0000
	Epibenthic:2014 – Epibenthic:2012	0.0001
	Epibenthic:2014 – Pelagic:2013	0.0008
	Epibenthic:2014 – Epibenthic:2013	0.0009
	Epibenthic:2014 – Pelagic:2014	0.0000
	Epibenthic:2014 – Epibenthic:2015	0.0001
Epibenthic:2014 – Pelagic:2015	0.0001	
<i>AMPHIPODS</i>	Epibenthic:2014 – Pelagic:2011	0.0060
	Epibenthic:2014 – Epibenthic:2011	0.0017
	Epibenthic:2014 – Pelagic:2012	0.0010
	Epibenthic:2014 – Epibenthic:2012	0.0014
	Epibenthic:2014 – Pelagic:2013	0.0101
	Epibenthic:2014 – Epibenthic:2013	0.0087
	Epibenthic:2014 – Pelagic:2014	0.0063
	Epibenthic:2014 – Pelagic:2015	0.0312
Epibenthic:2014 – Epibenthic:2015	0.0010	

793 Table 4. GAM model significant terms for each taxon with R^2 and the percentage of deviance
 794 explained. * $p < 0.05$; ** $p < 0.01$; *** $p < 0.001$

	Significant terms	R^2	Deviance explained
<i>Calanus glacialis</i> C5	Surface Salinity*** Surface Temperature* 14-day Transport* Bottom Temperature*** Ordinal Day*** Year***	0.394	43%
<i>Calanus glacialis</i> C2	Mean Bottom Temperature*** Mean Surface Temperature** Longitude* Julian Day* Year*	0.551	57%
<i>Thysanoessa raschii</i>	Mean Bottom Temperature** 30-day Transport* Longitude*** Ordinal Day ***	0.375	42.3%
<i>Euphausiid furcilia</i>	Mean Bottom Temperature *** 14-day Transport*** Longitude*** Ordinal Day*** Year***	0.53	55.8%

795

796

797

798

799

800

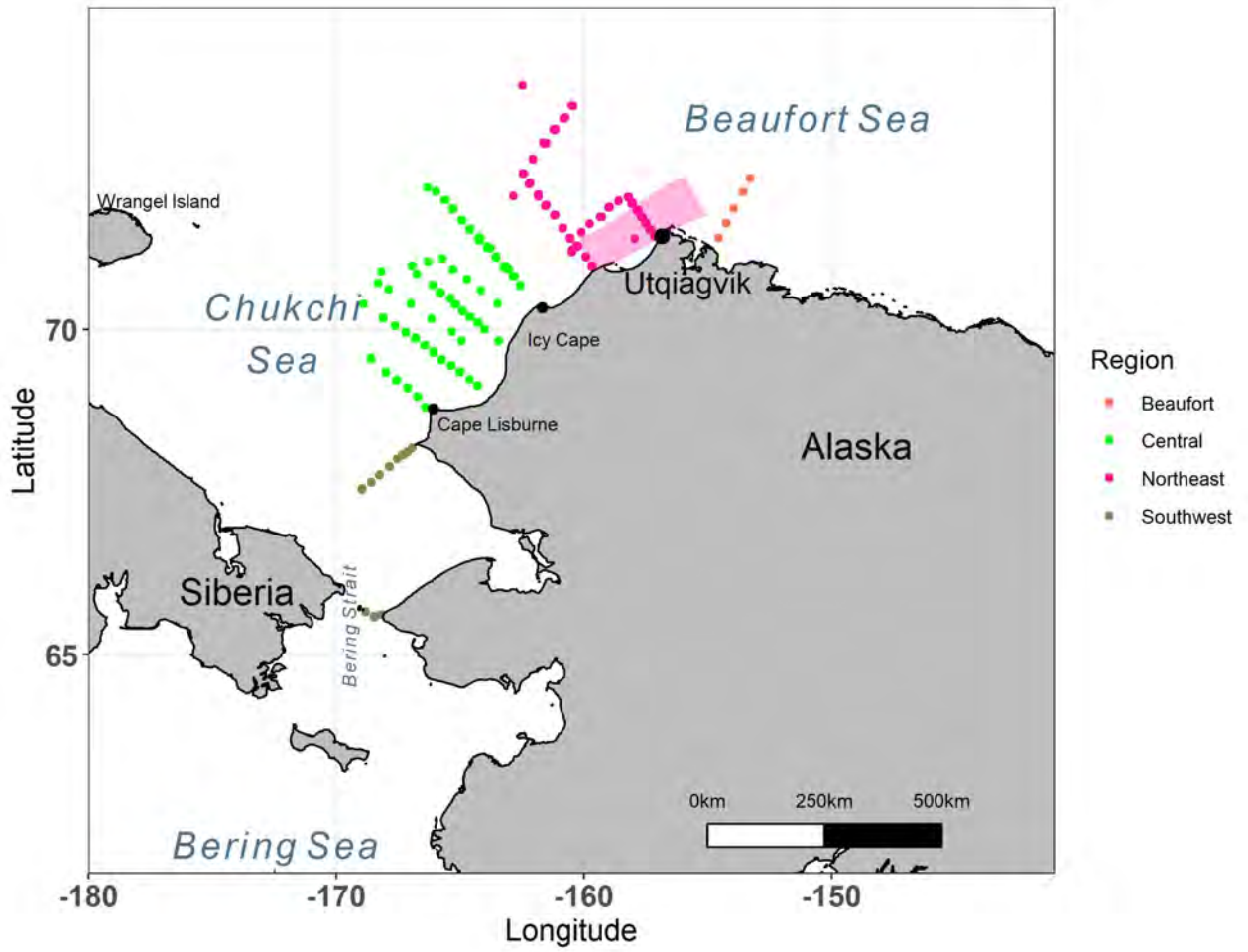
801

802

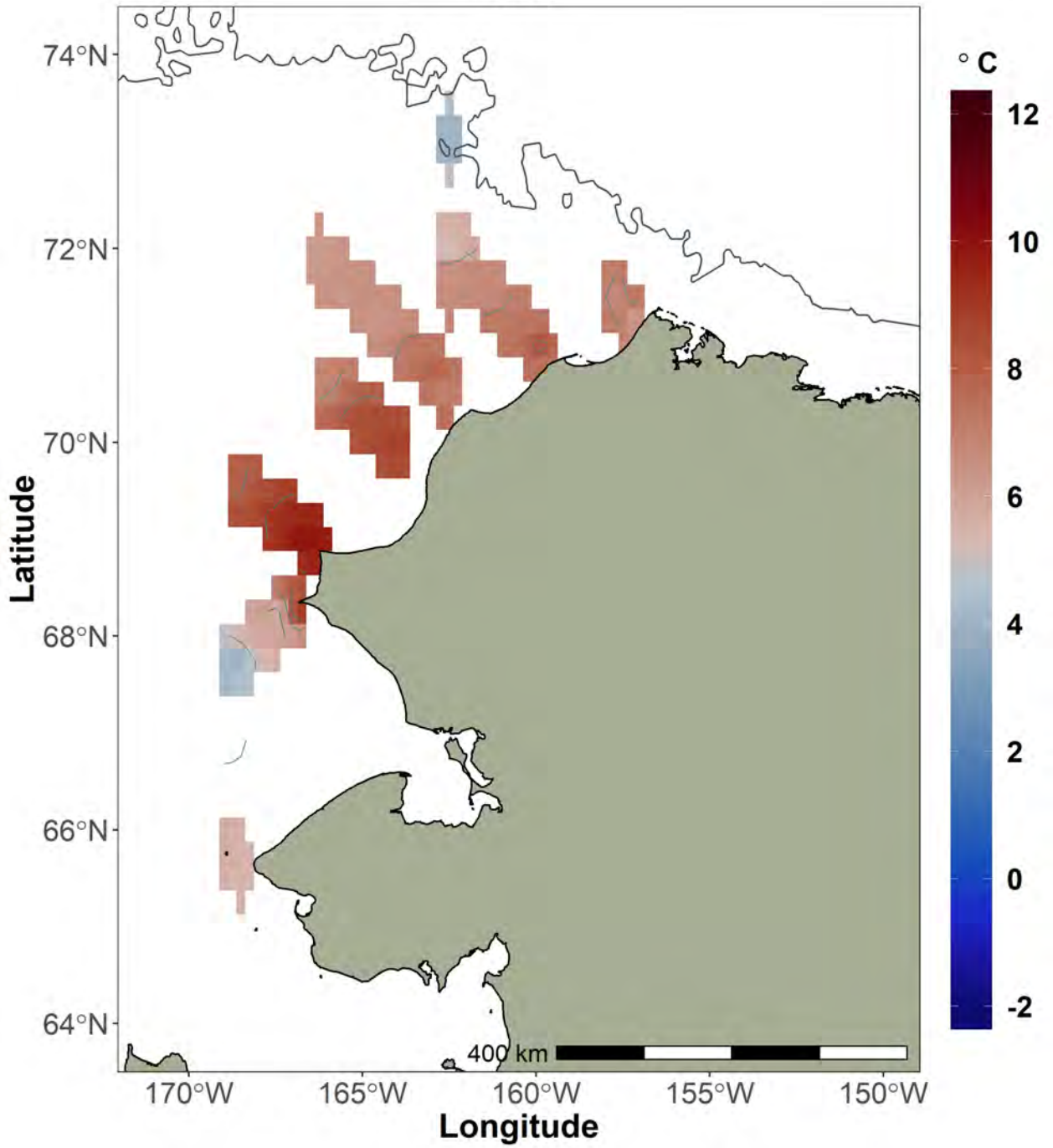
803

804

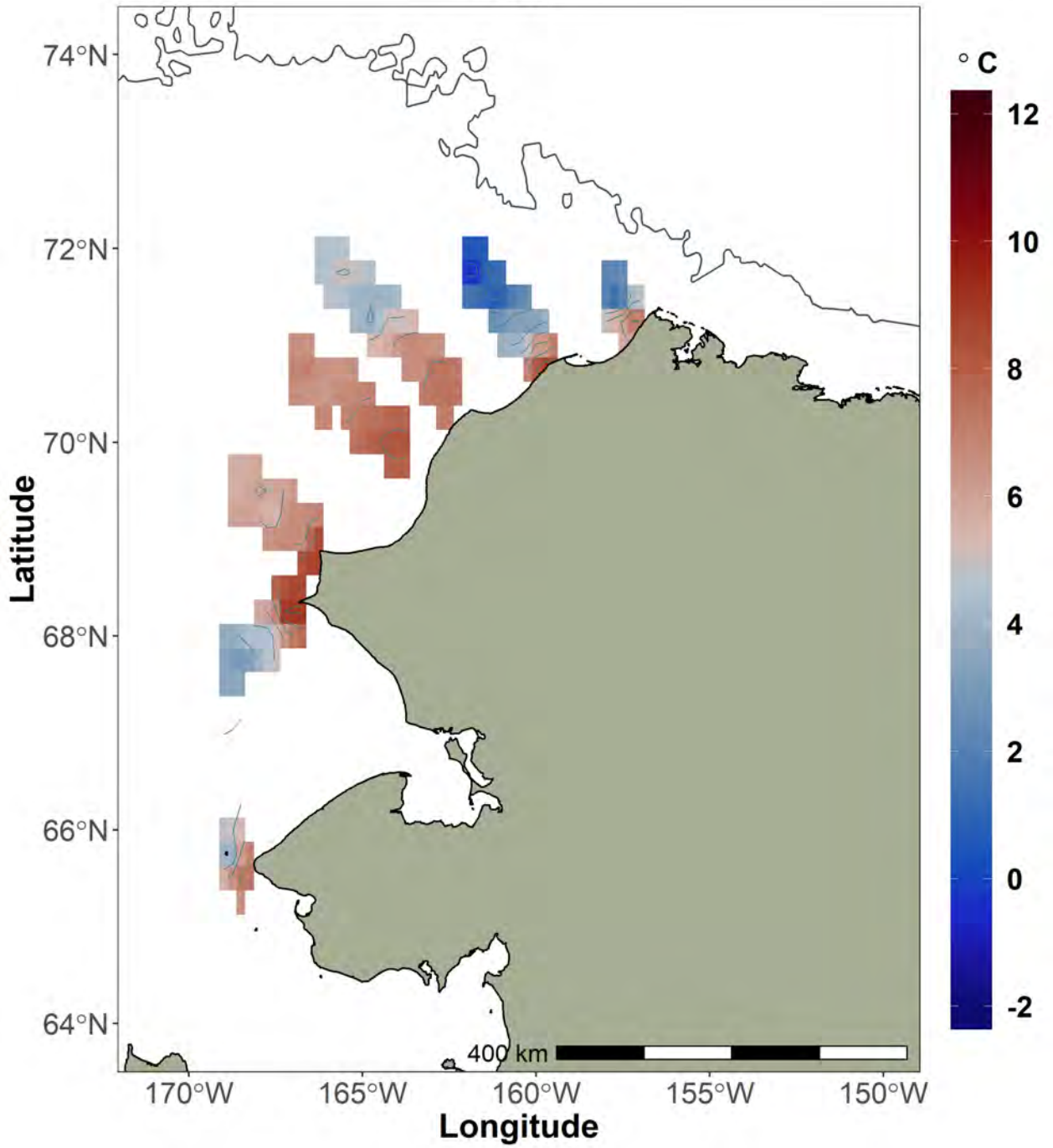
805



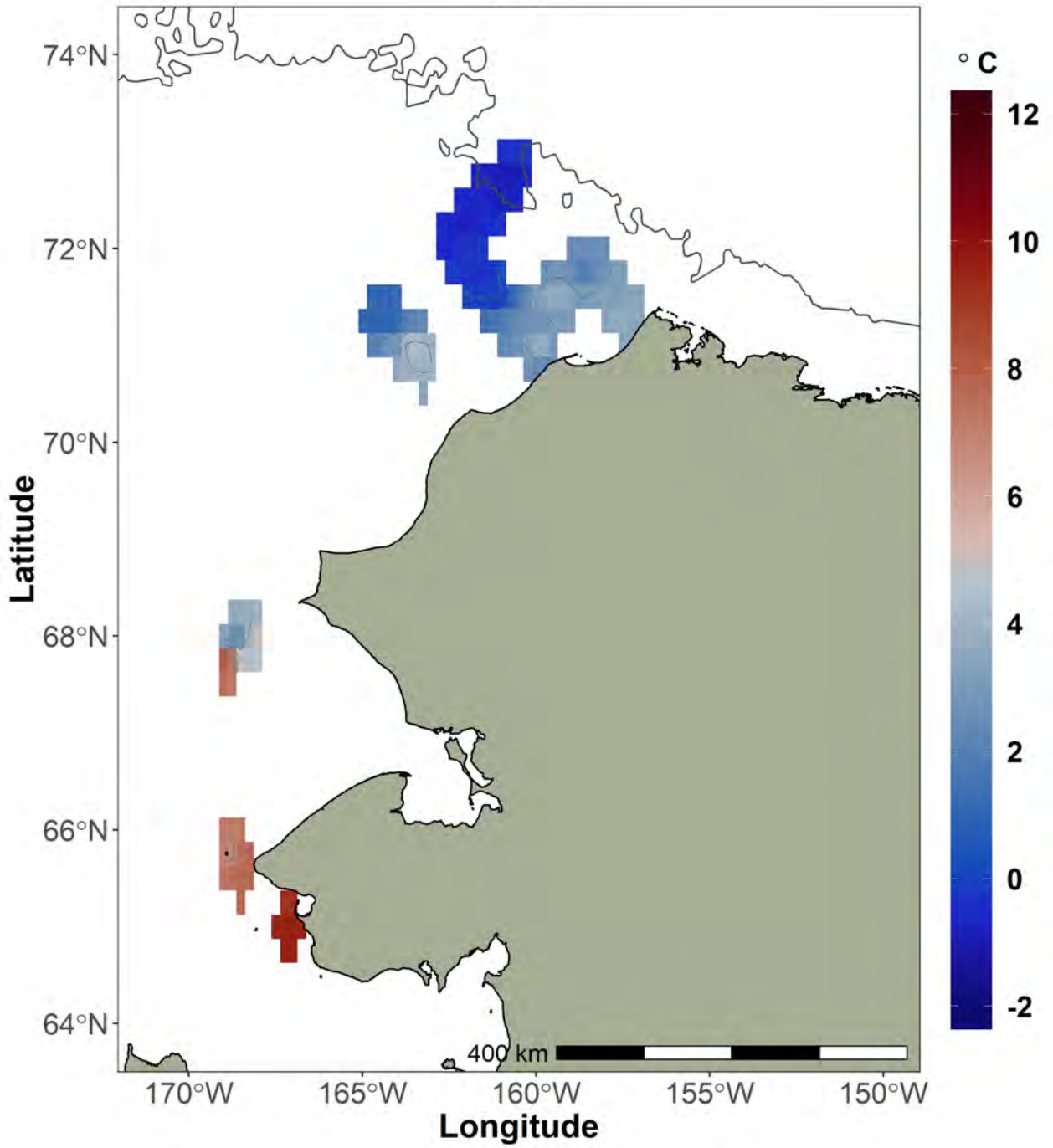
2011



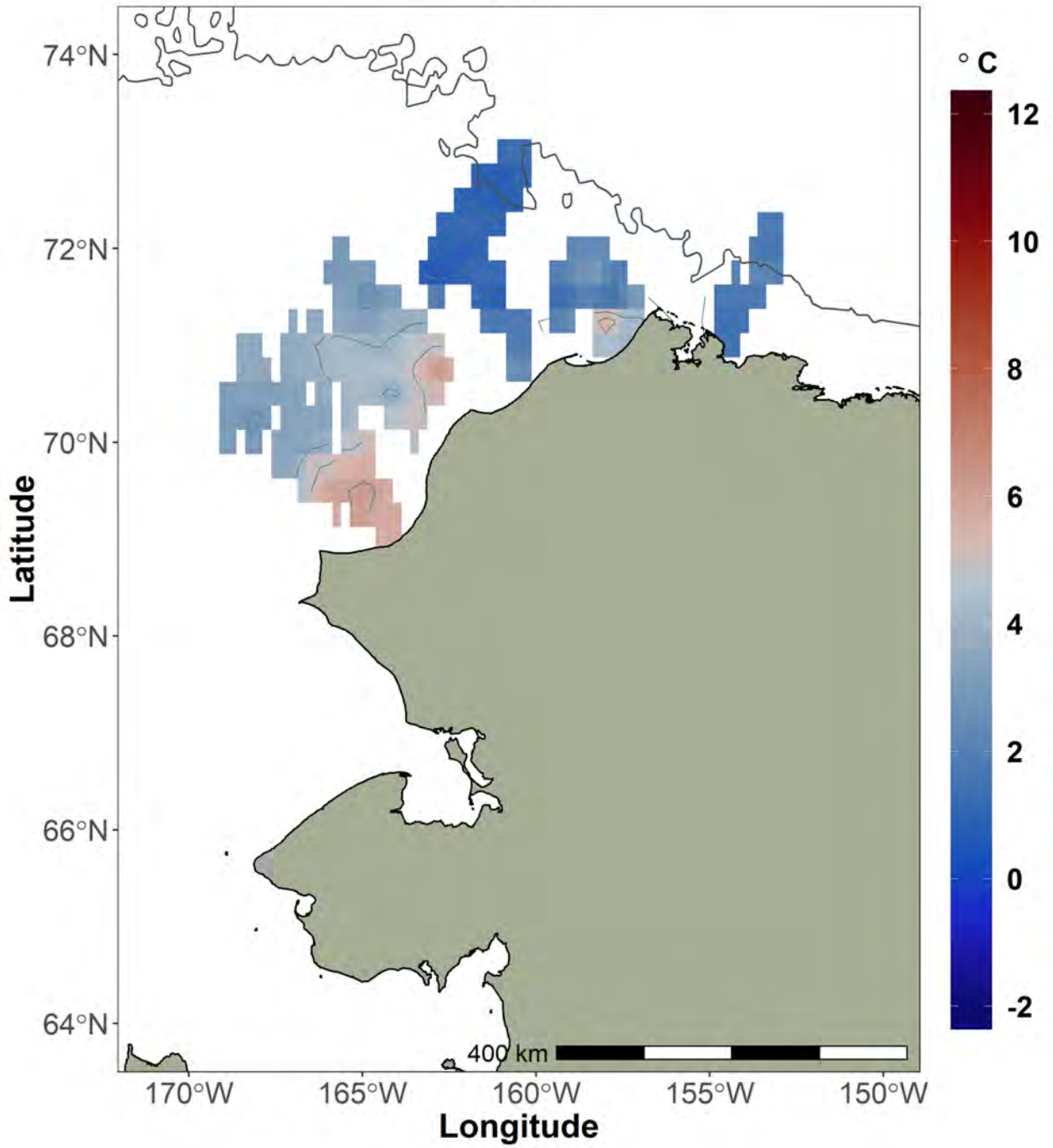
2012



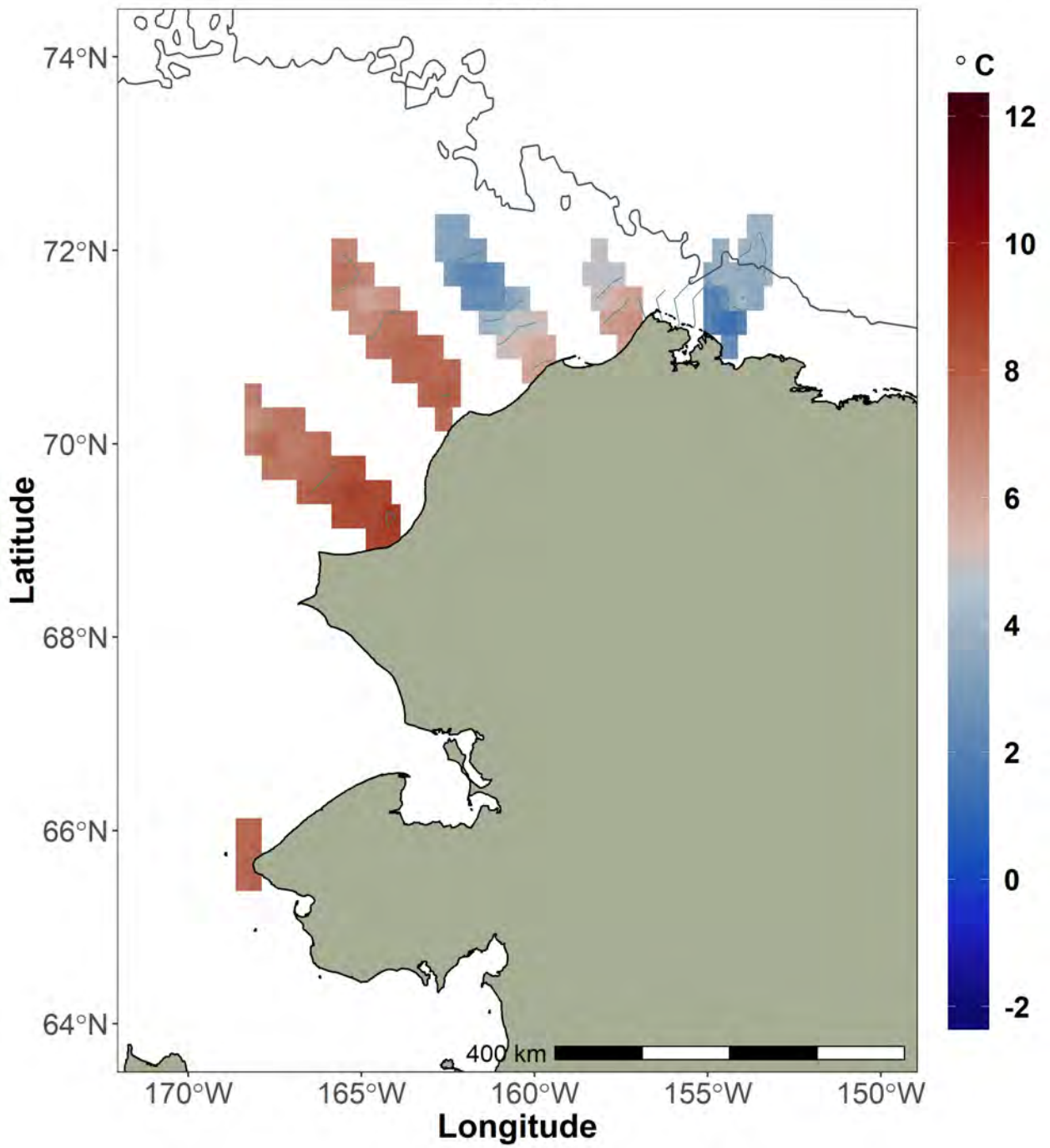
2013

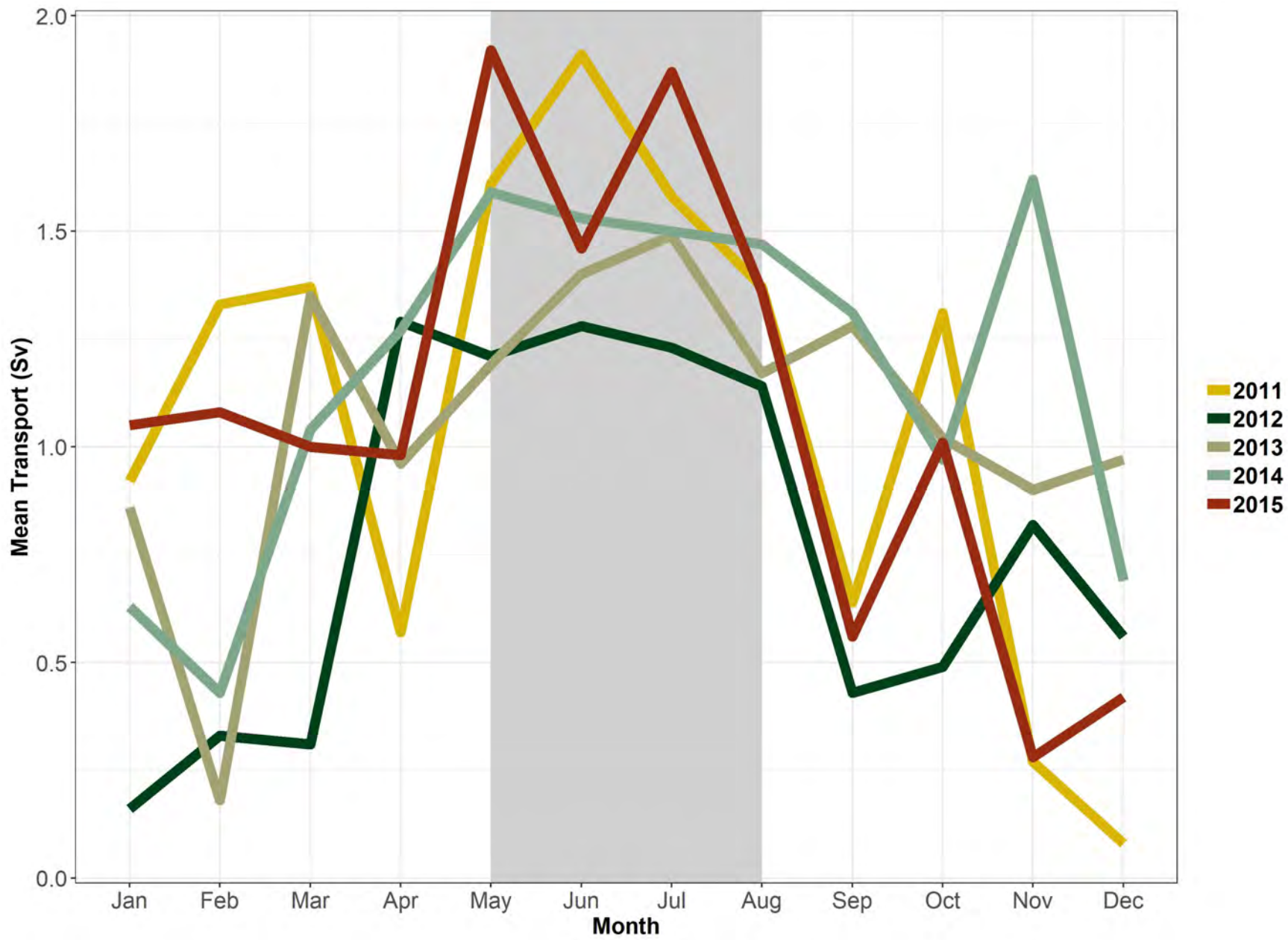


2014

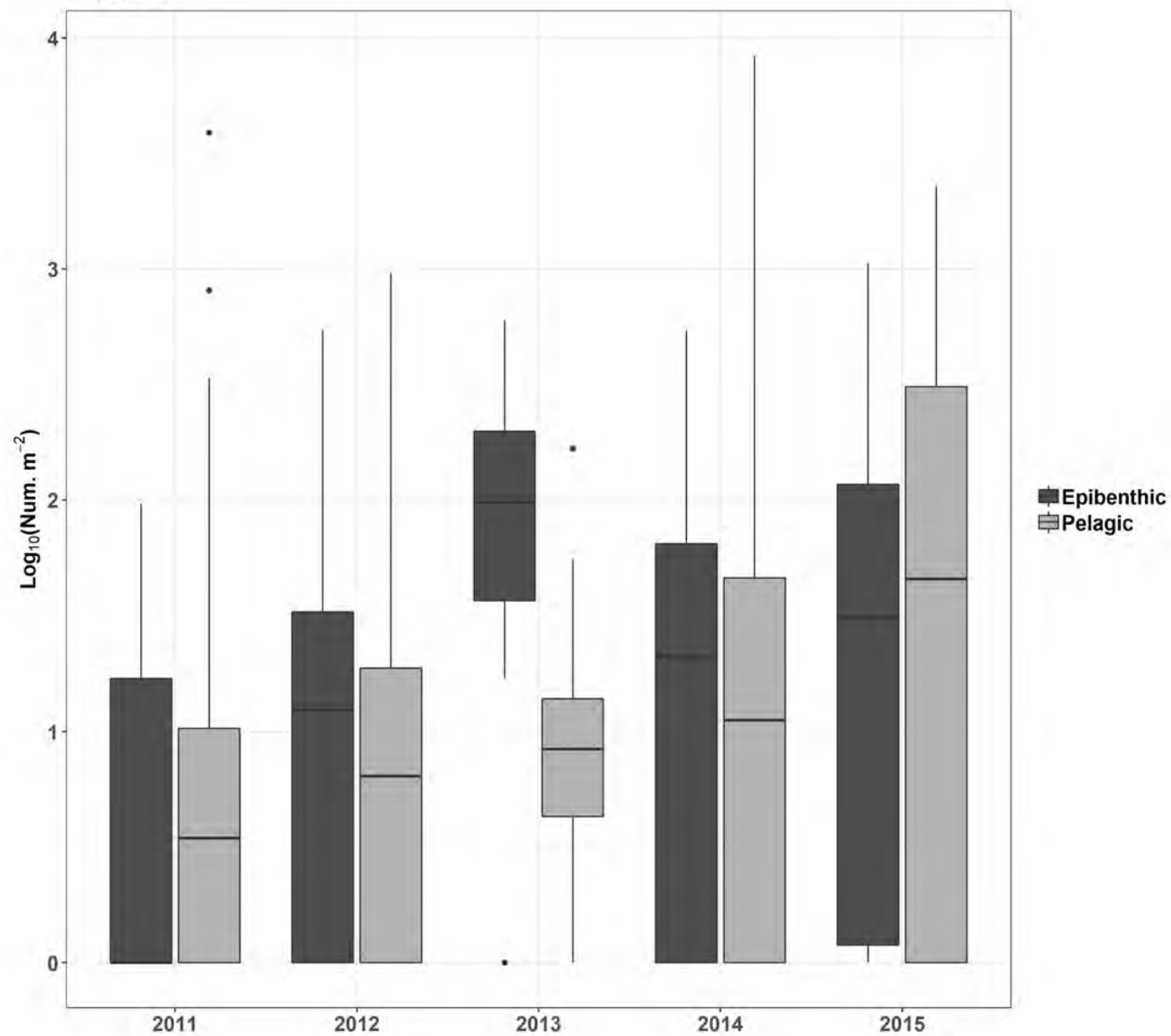


2015

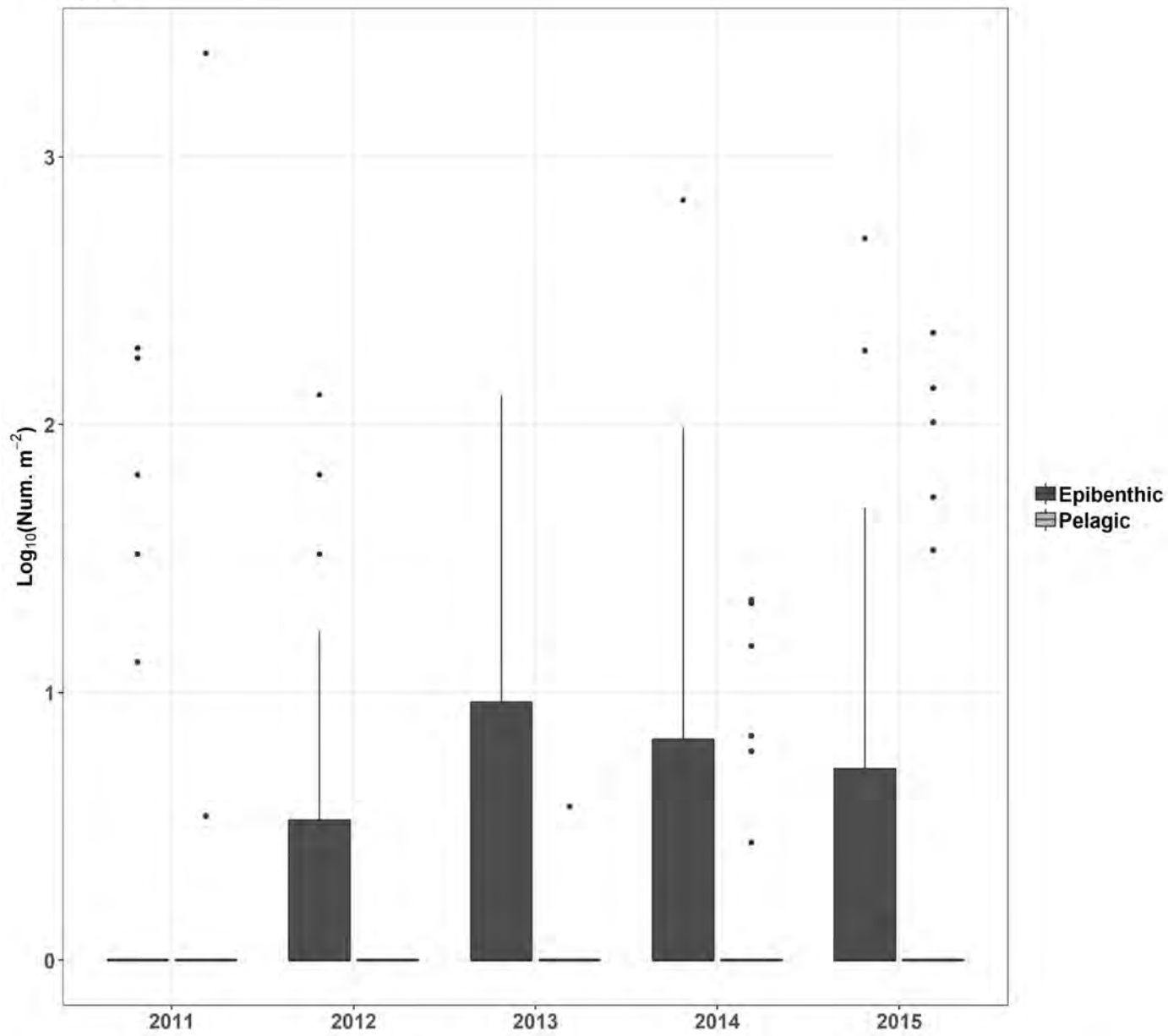




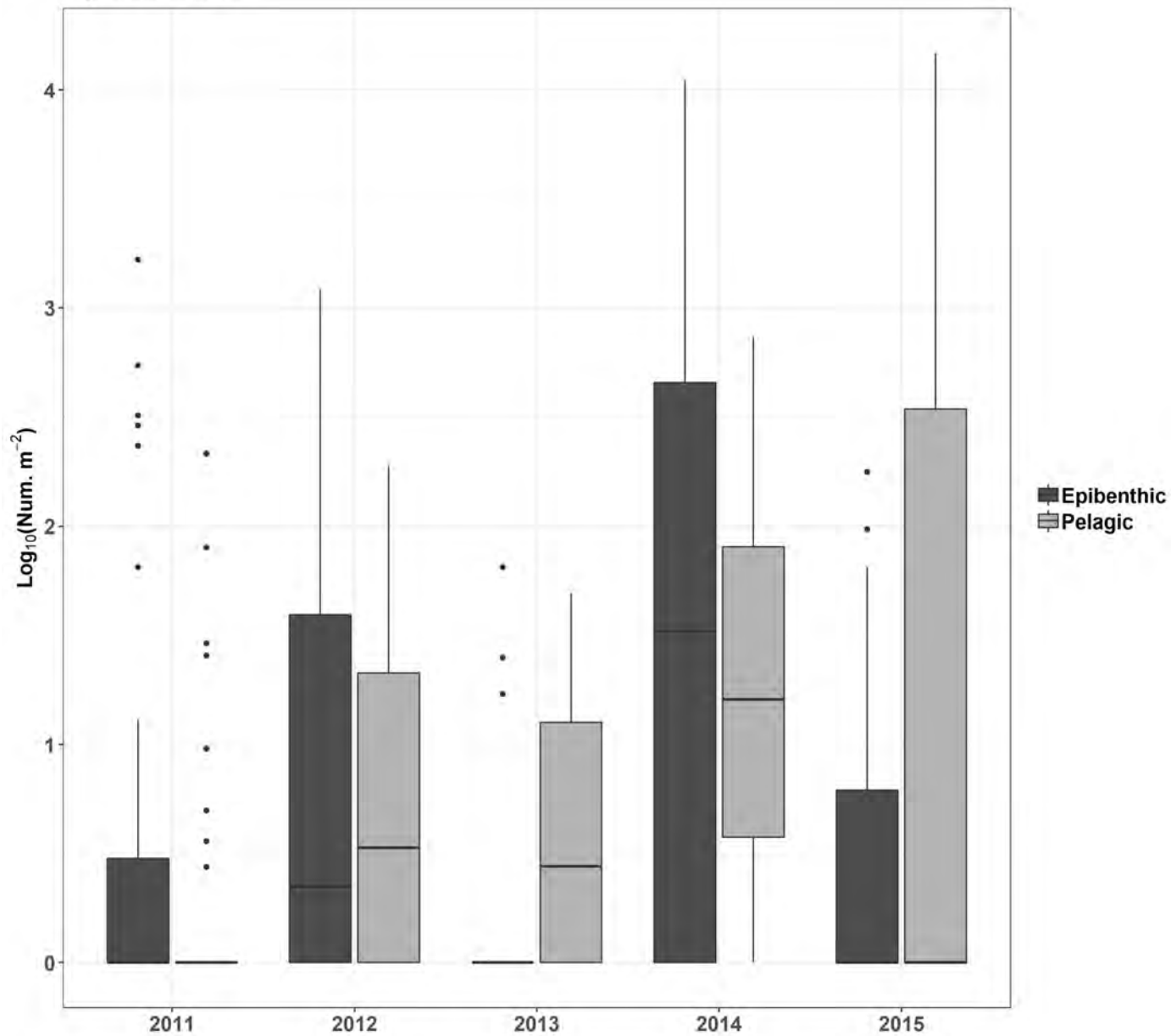
Amphipods



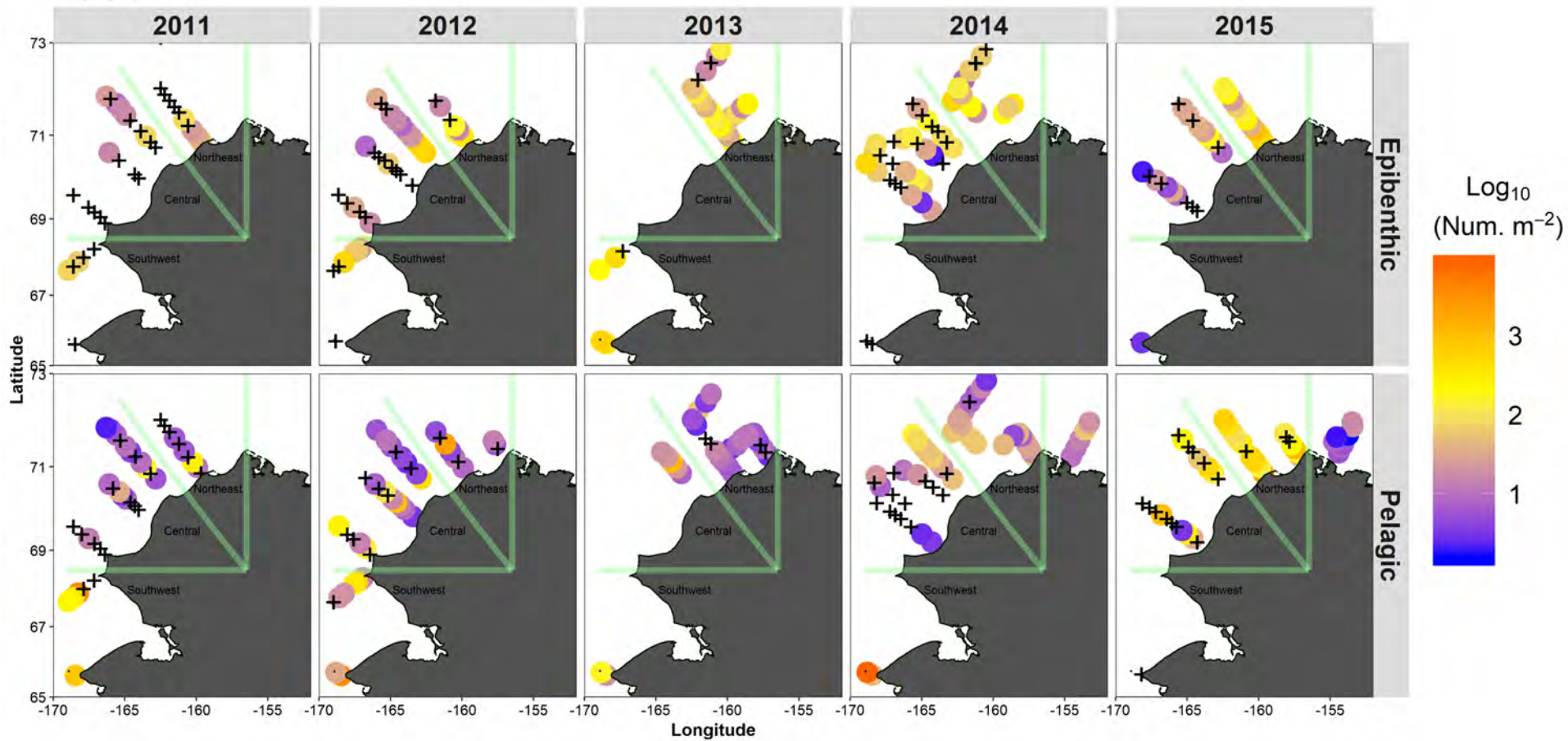
Mysids



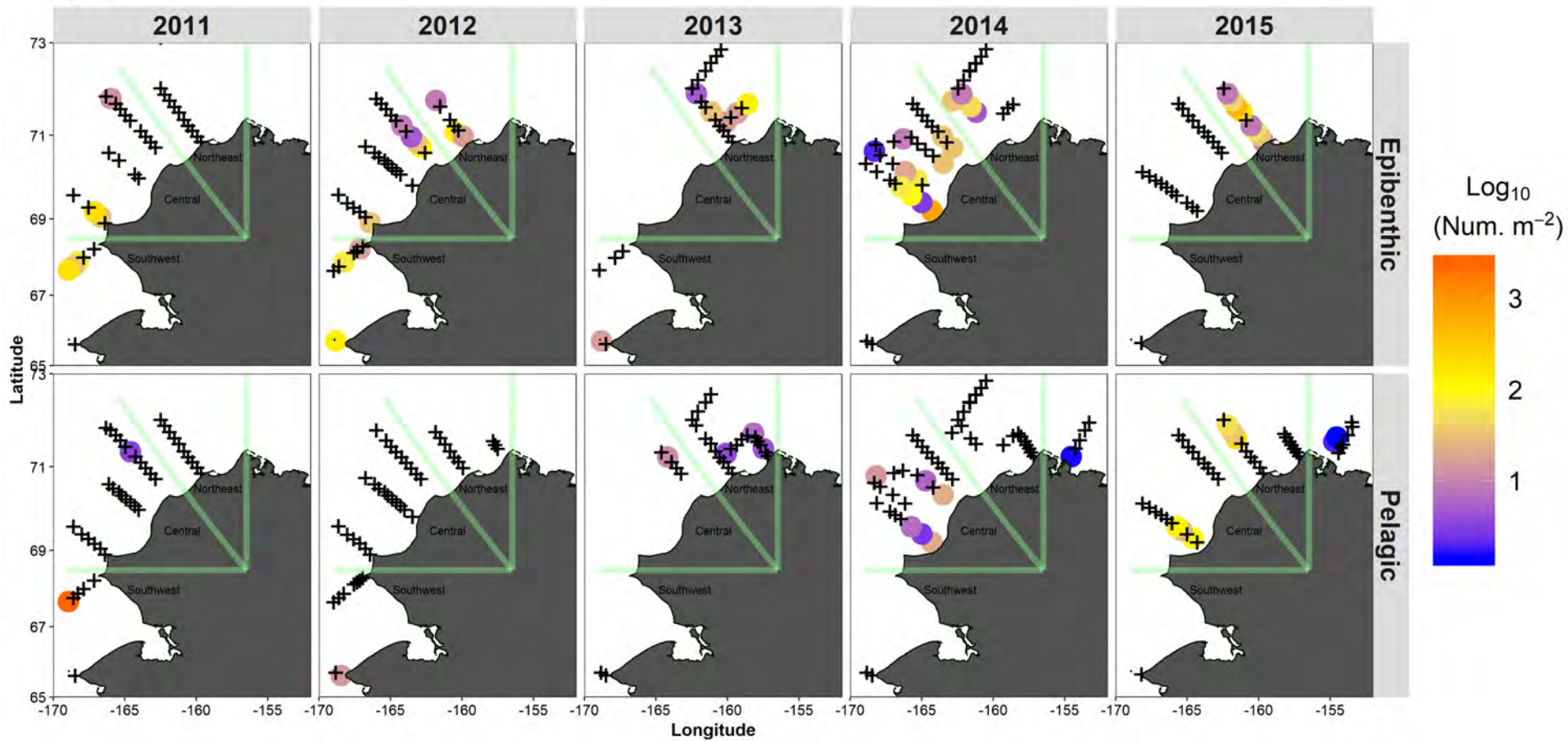
Thysanoessa raschii



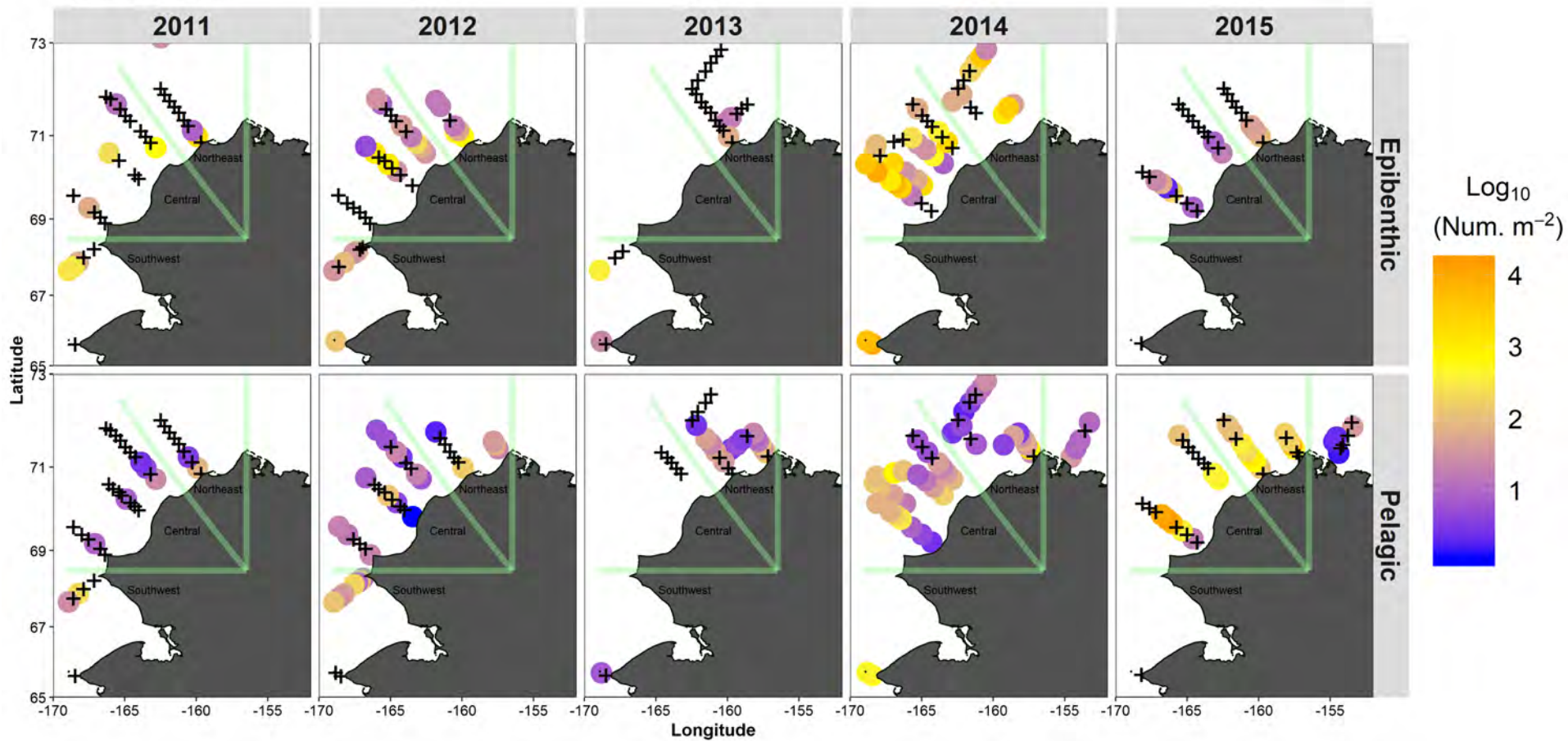
Amphipods



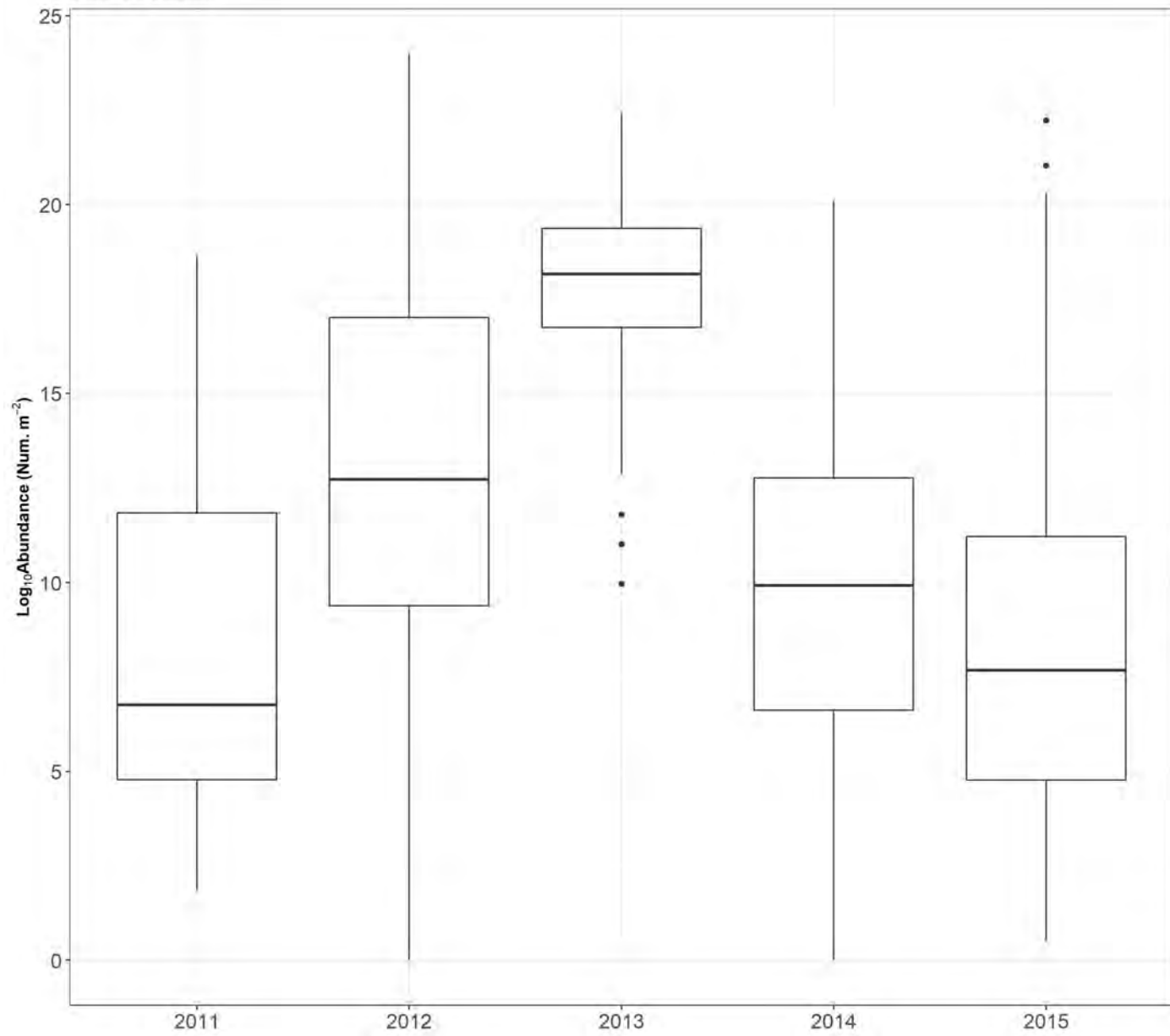
Mysids



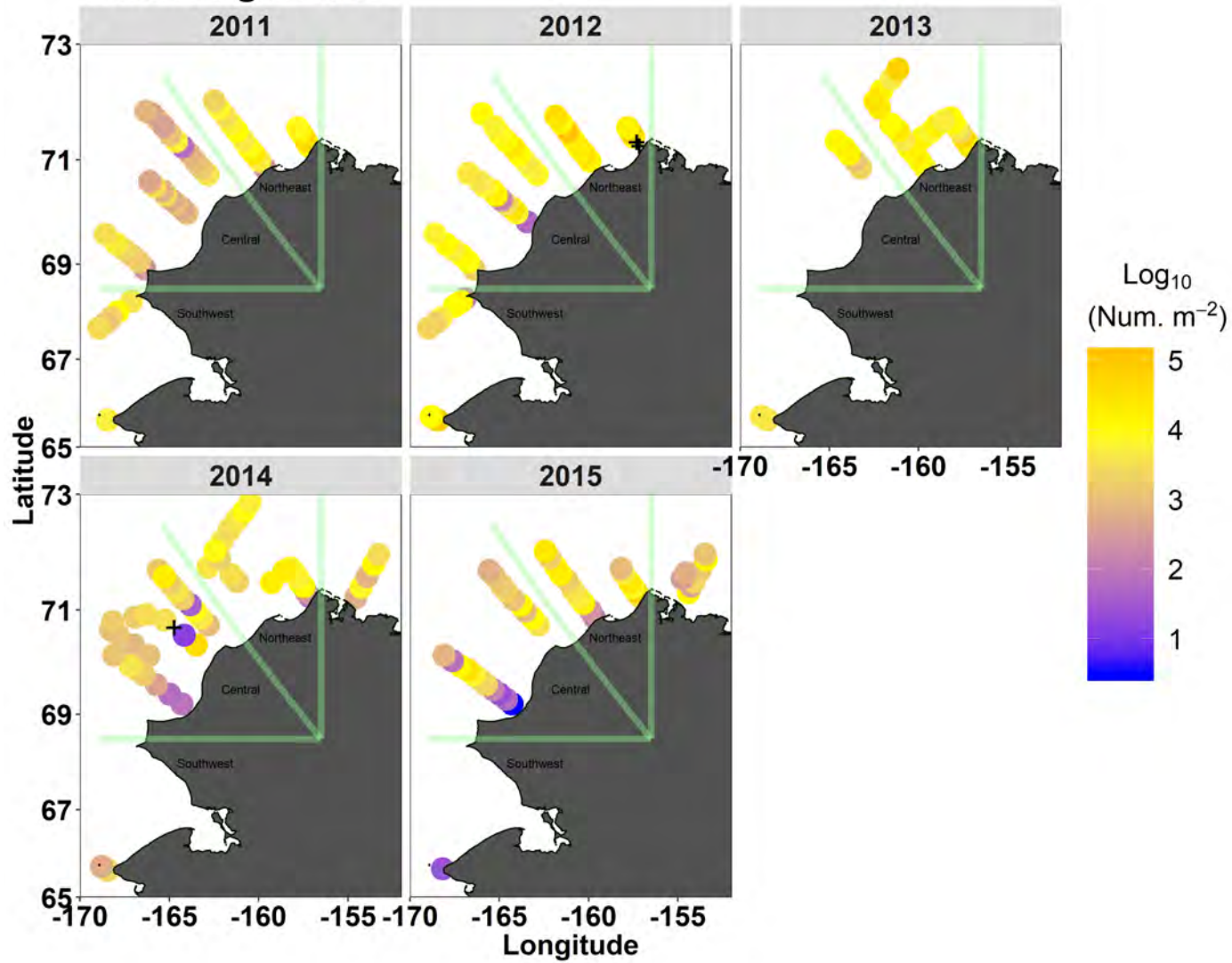
Thysanoessa raschii



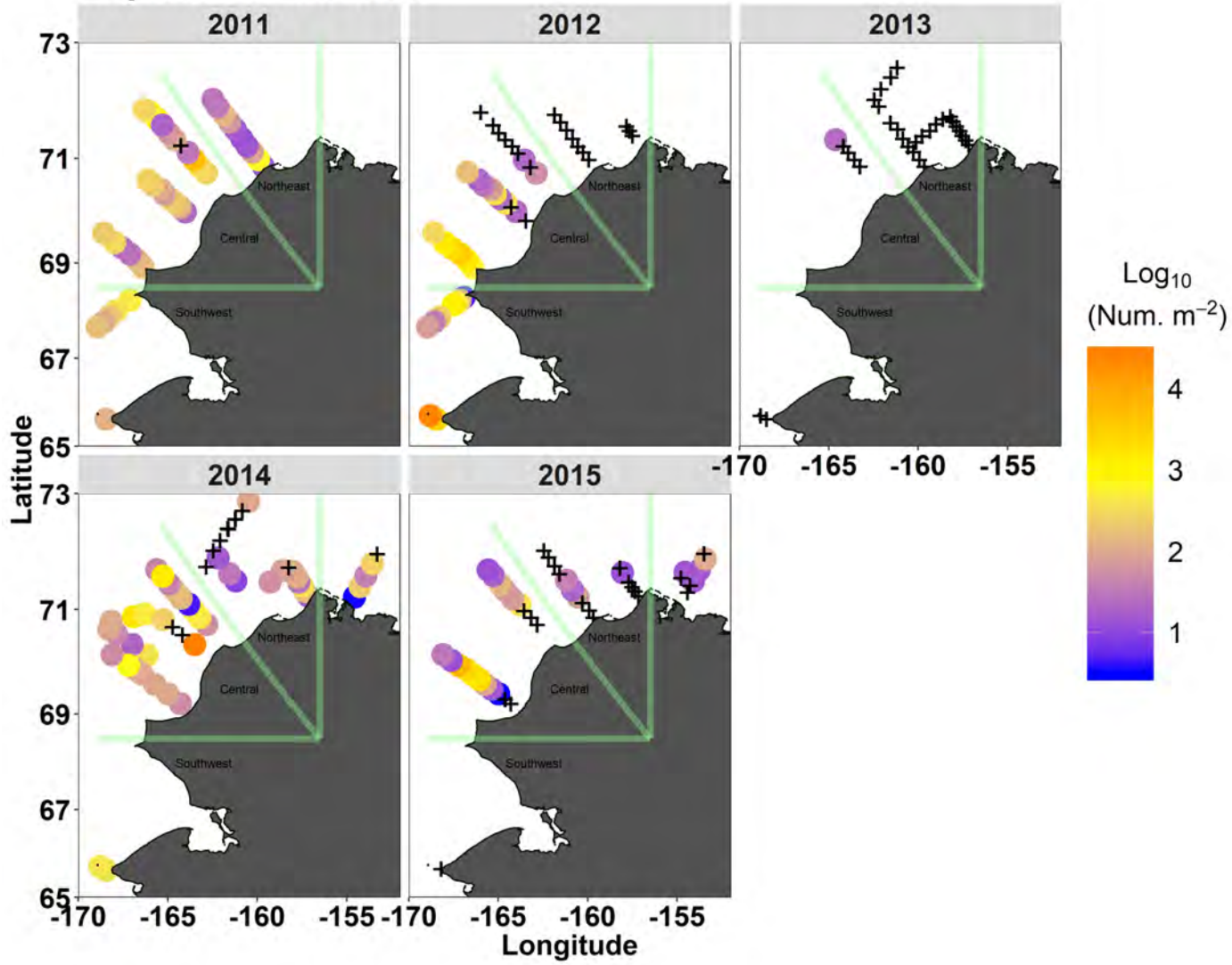
Calanus glacialis



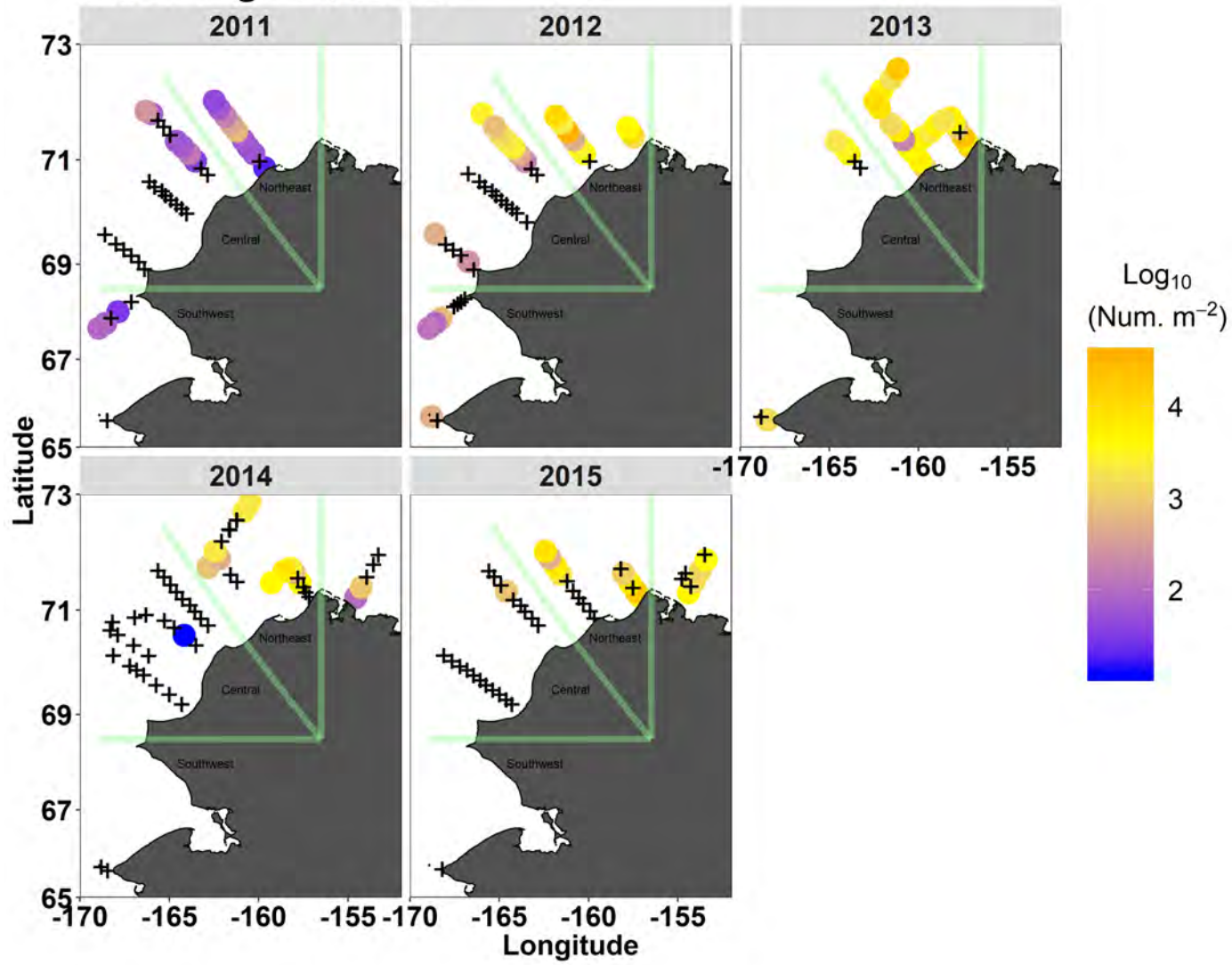
Calanus glacialis

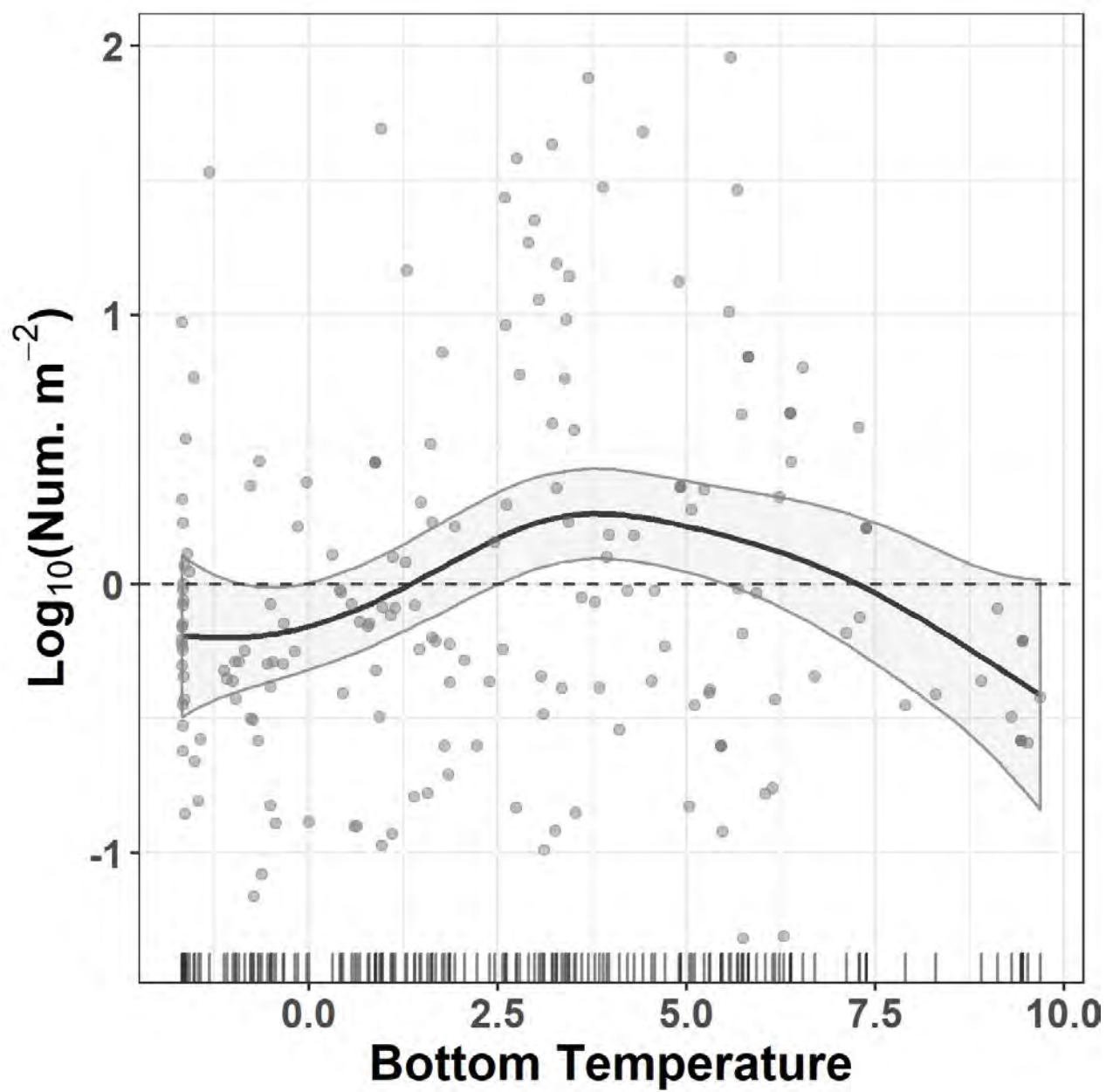


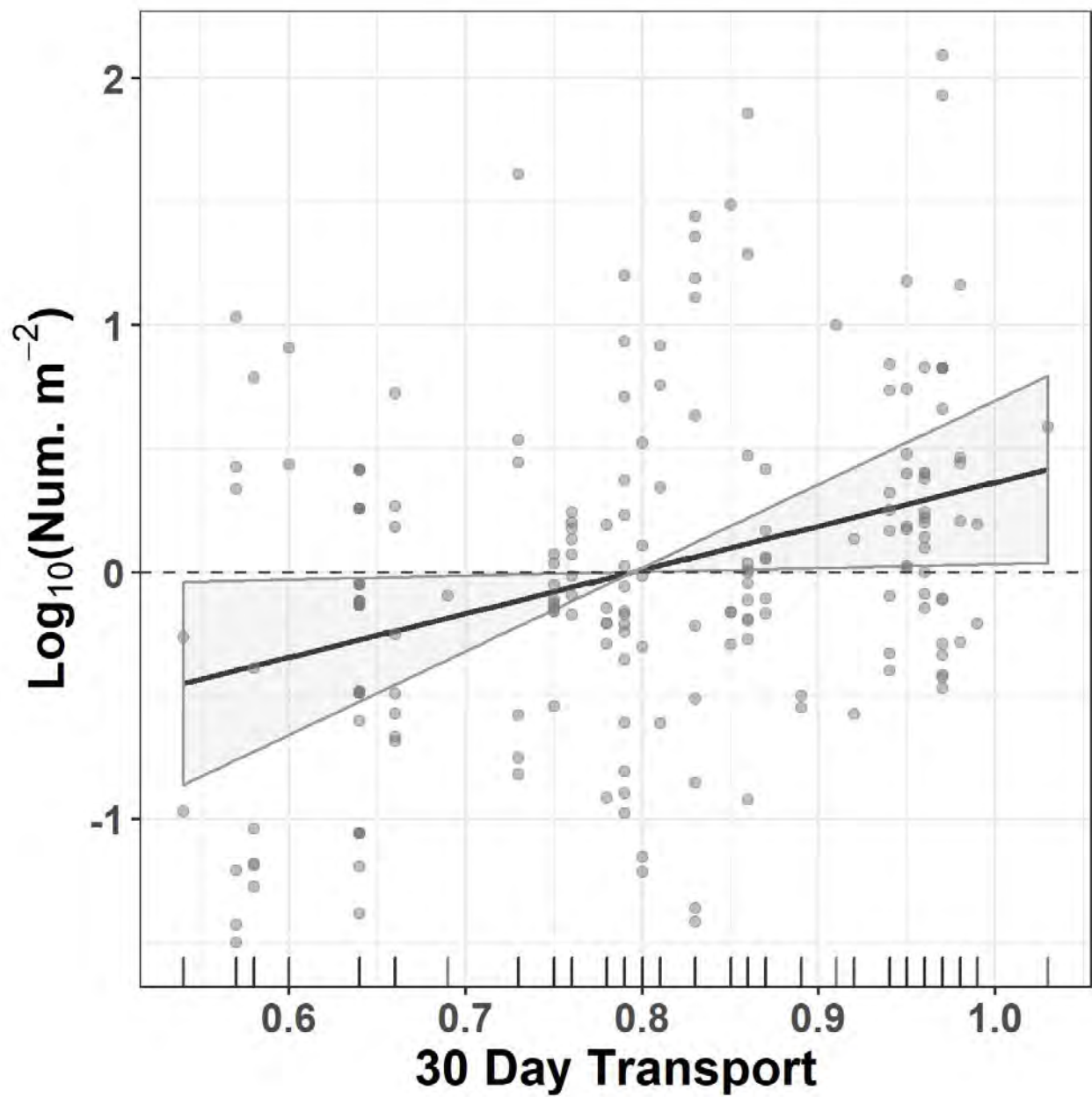
Euphausiid furcilia

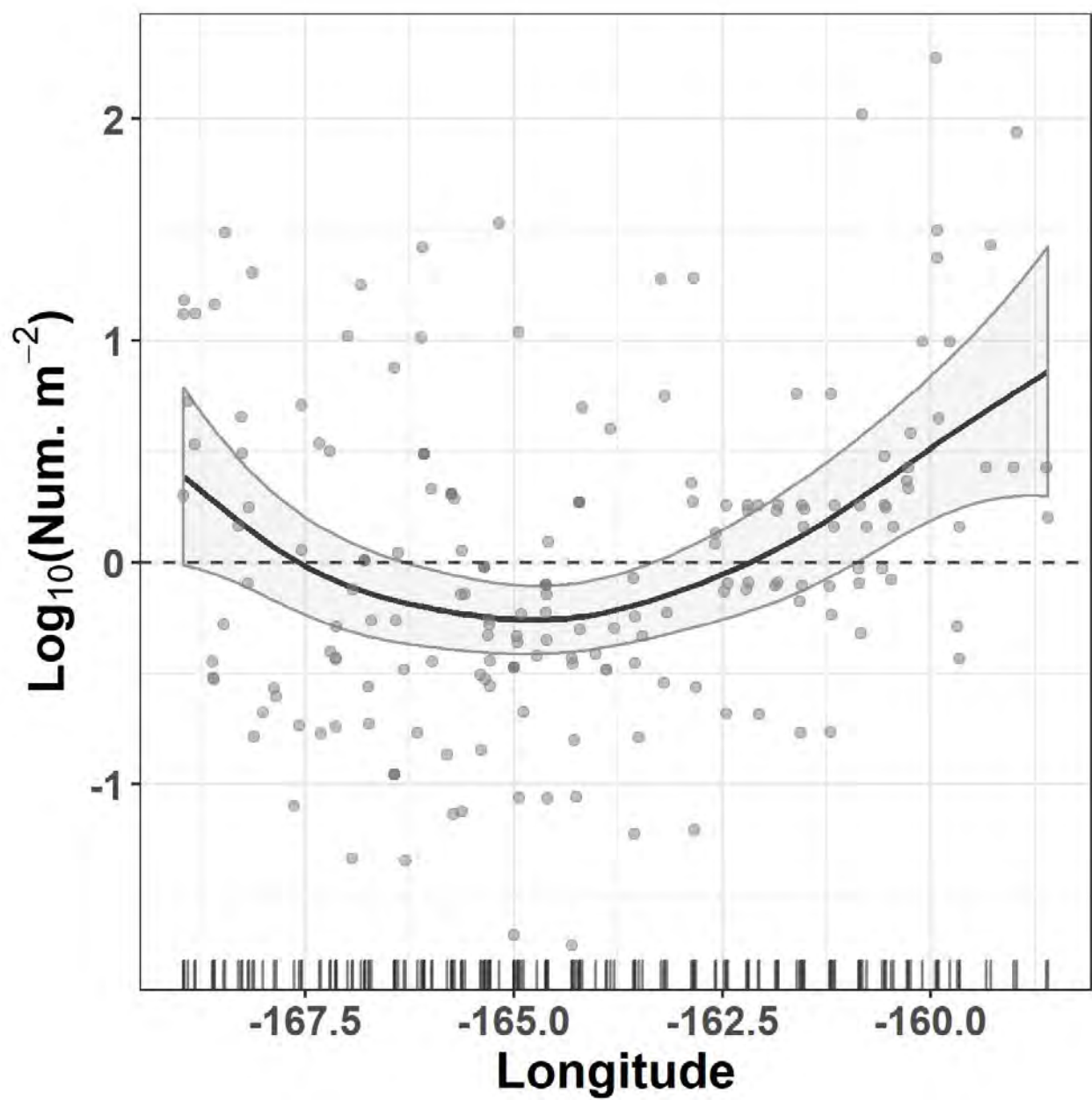


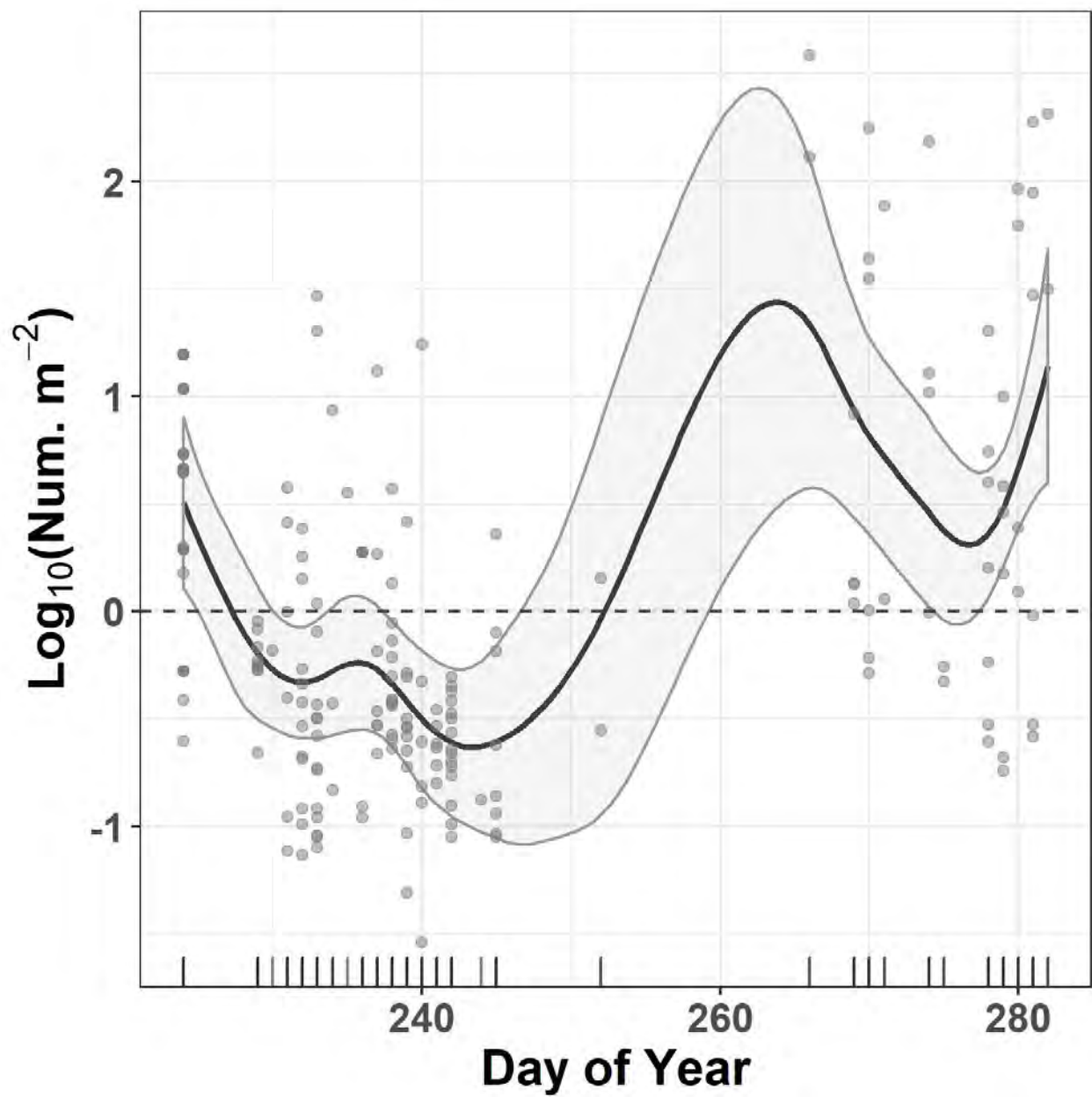
Calanus glacialis C2

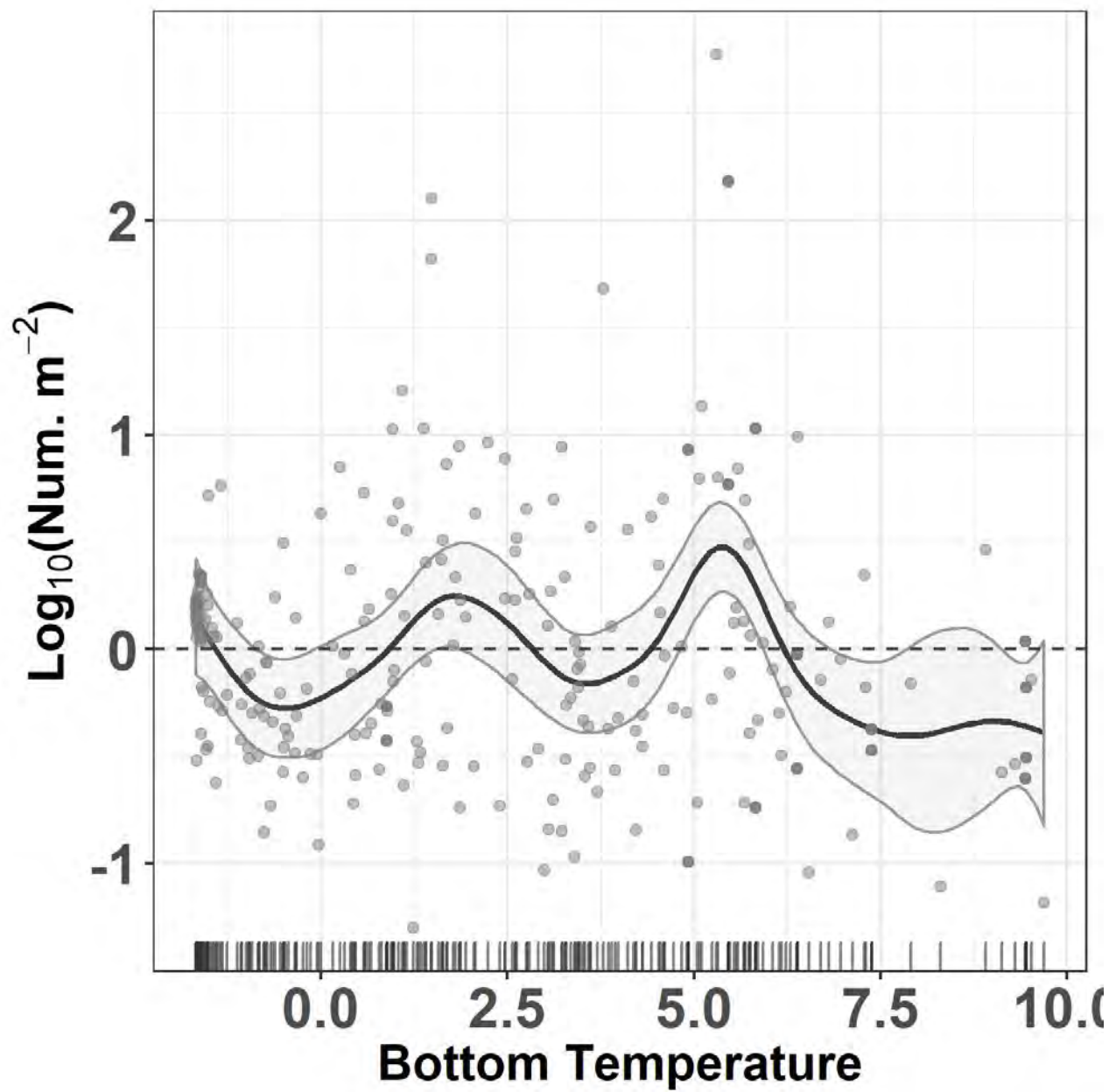


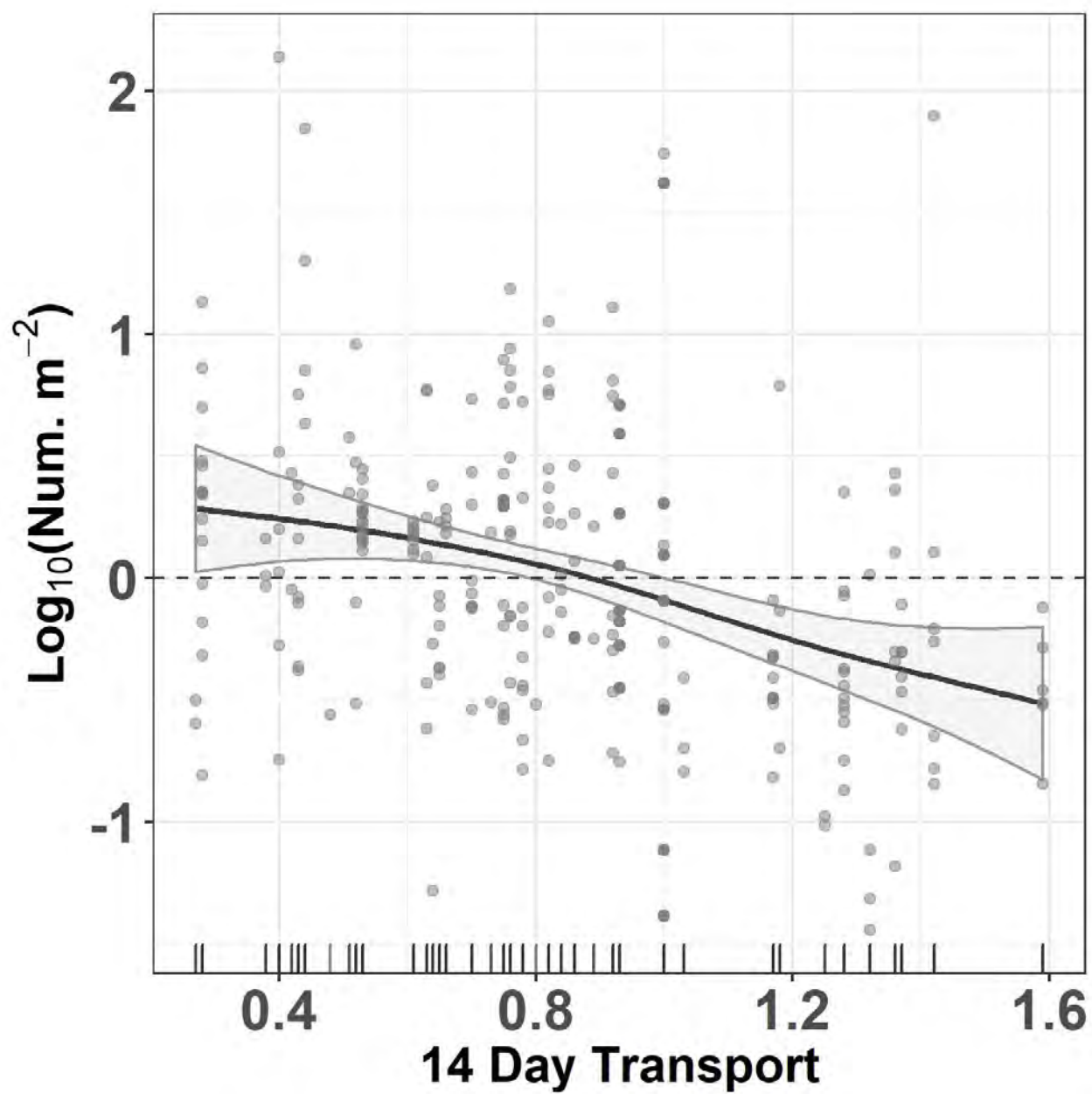


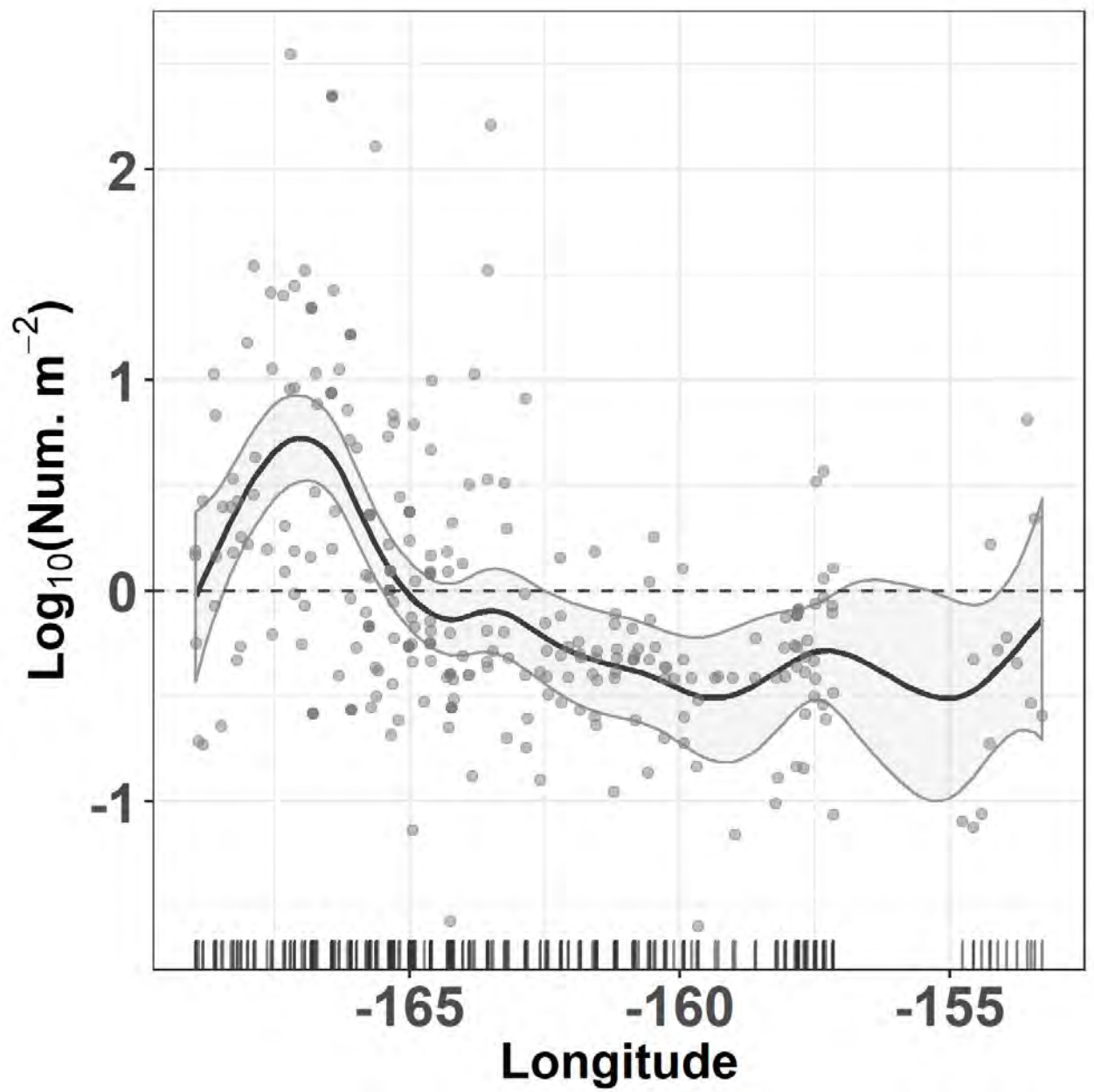


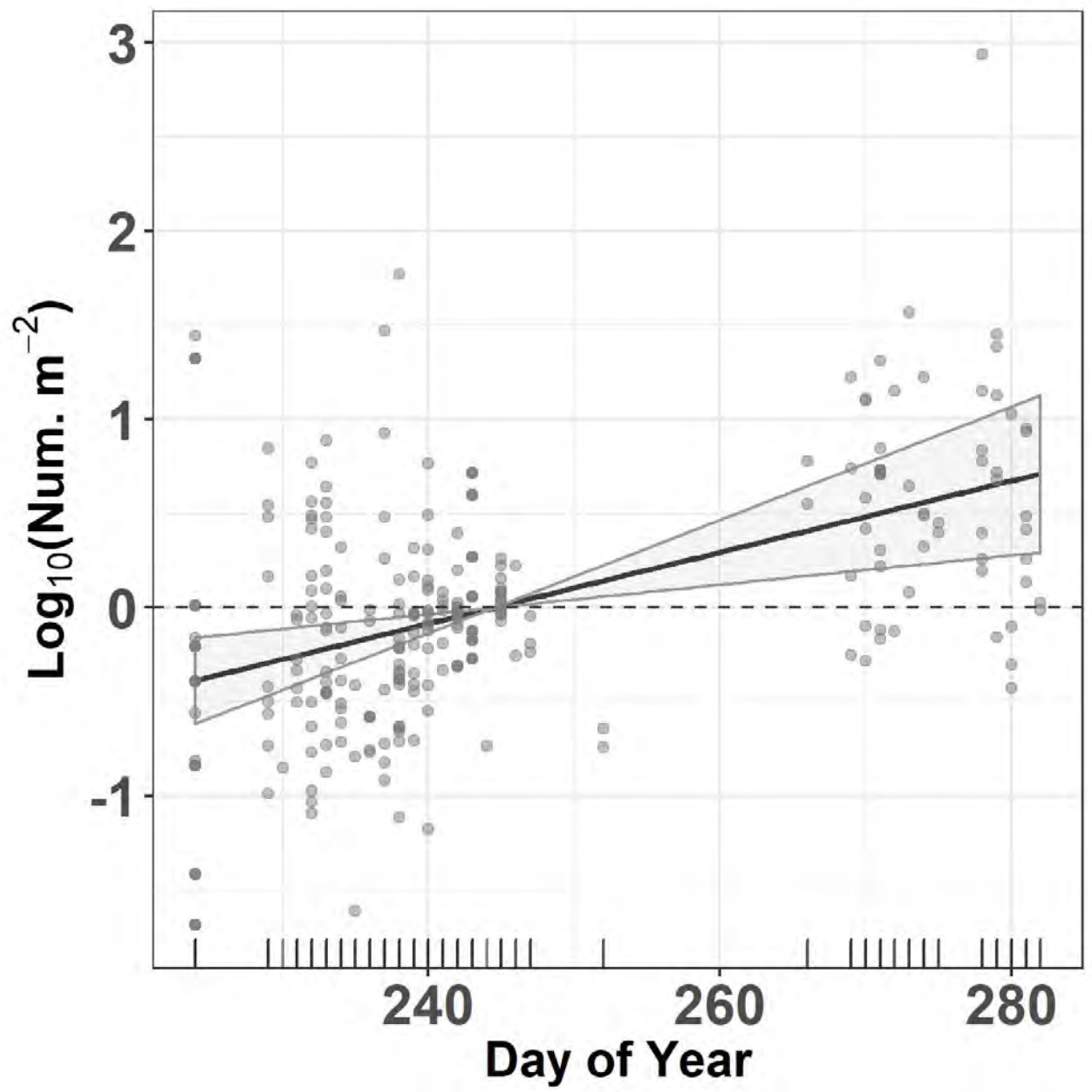


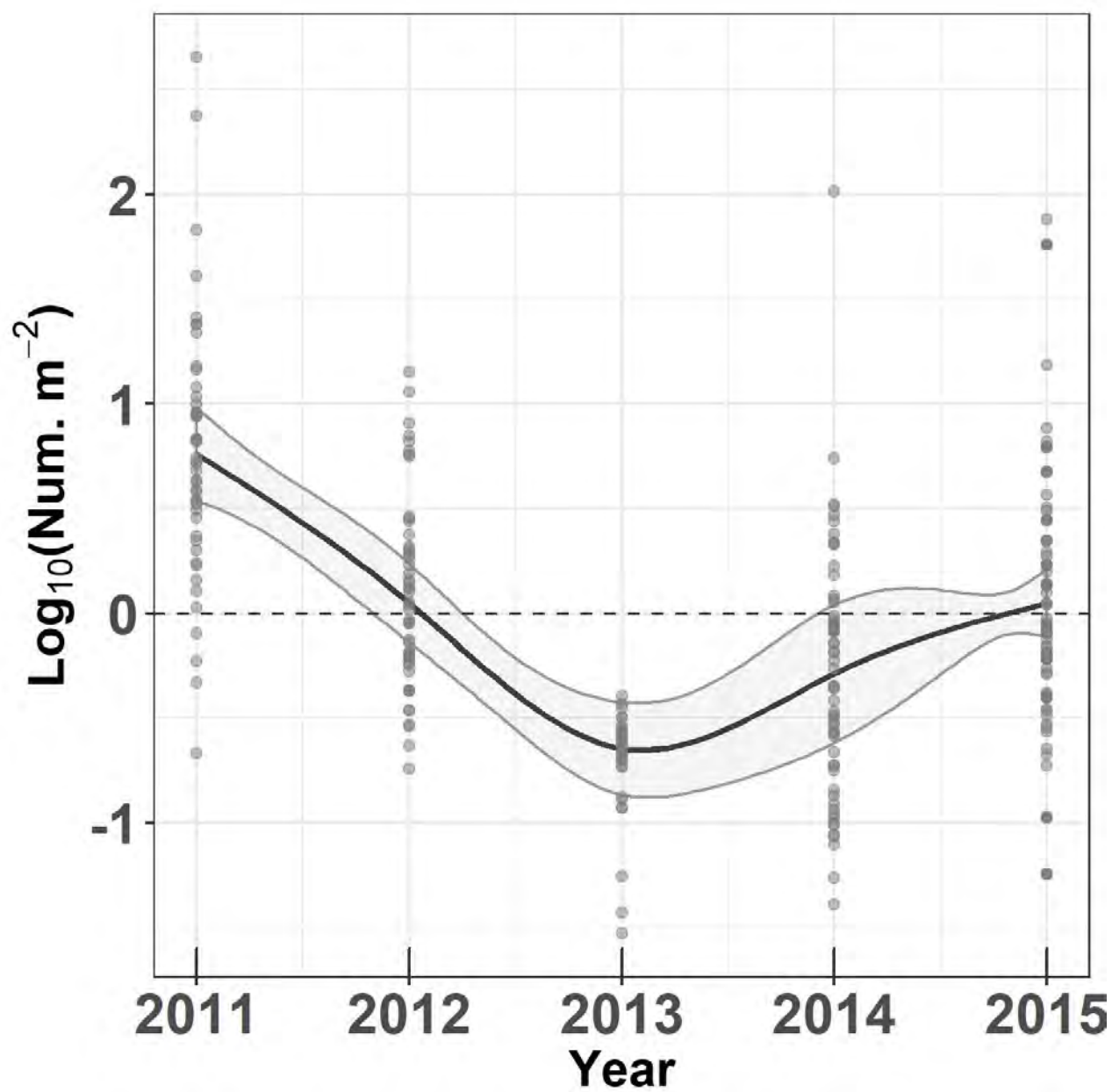


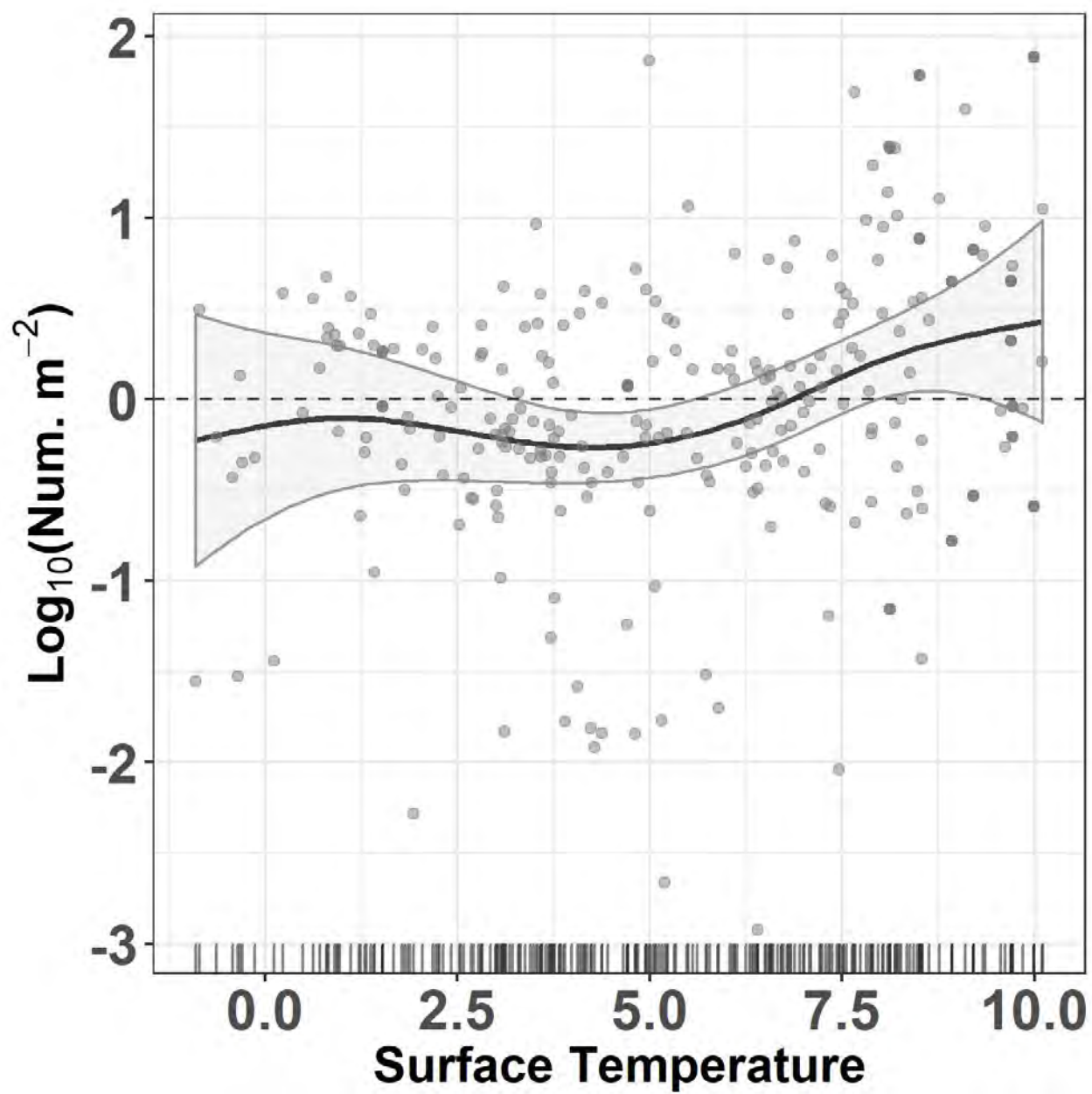


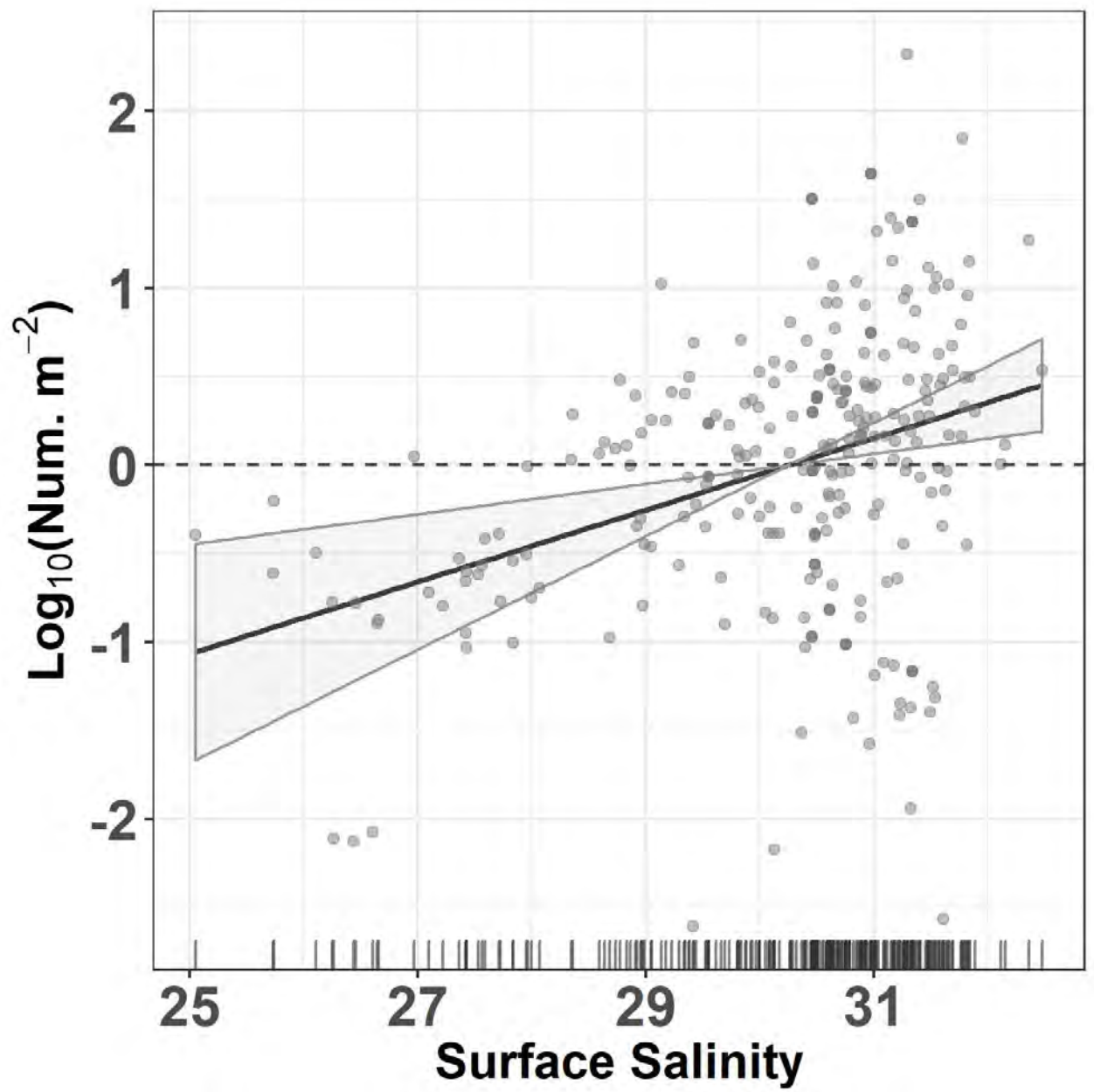


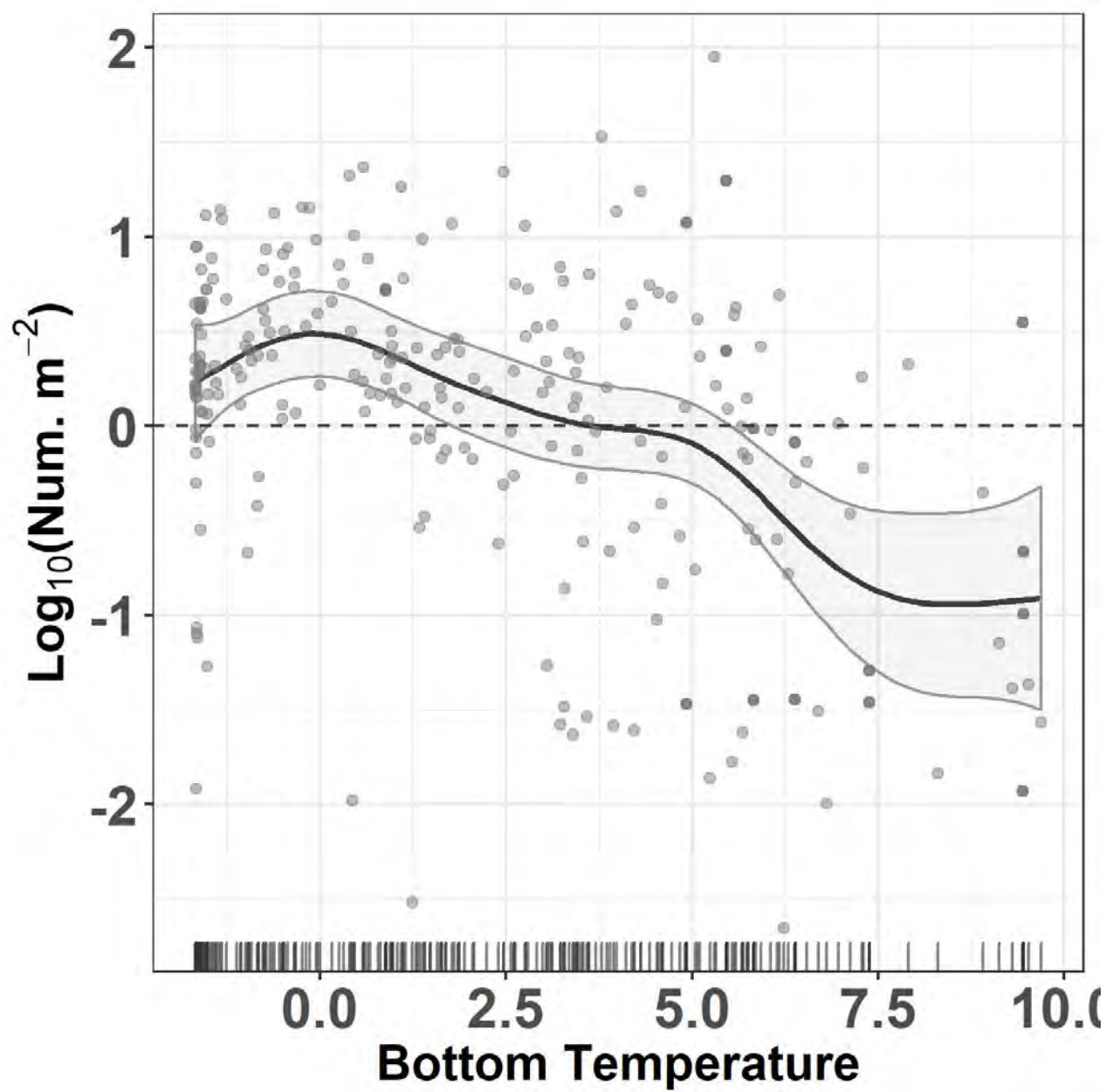


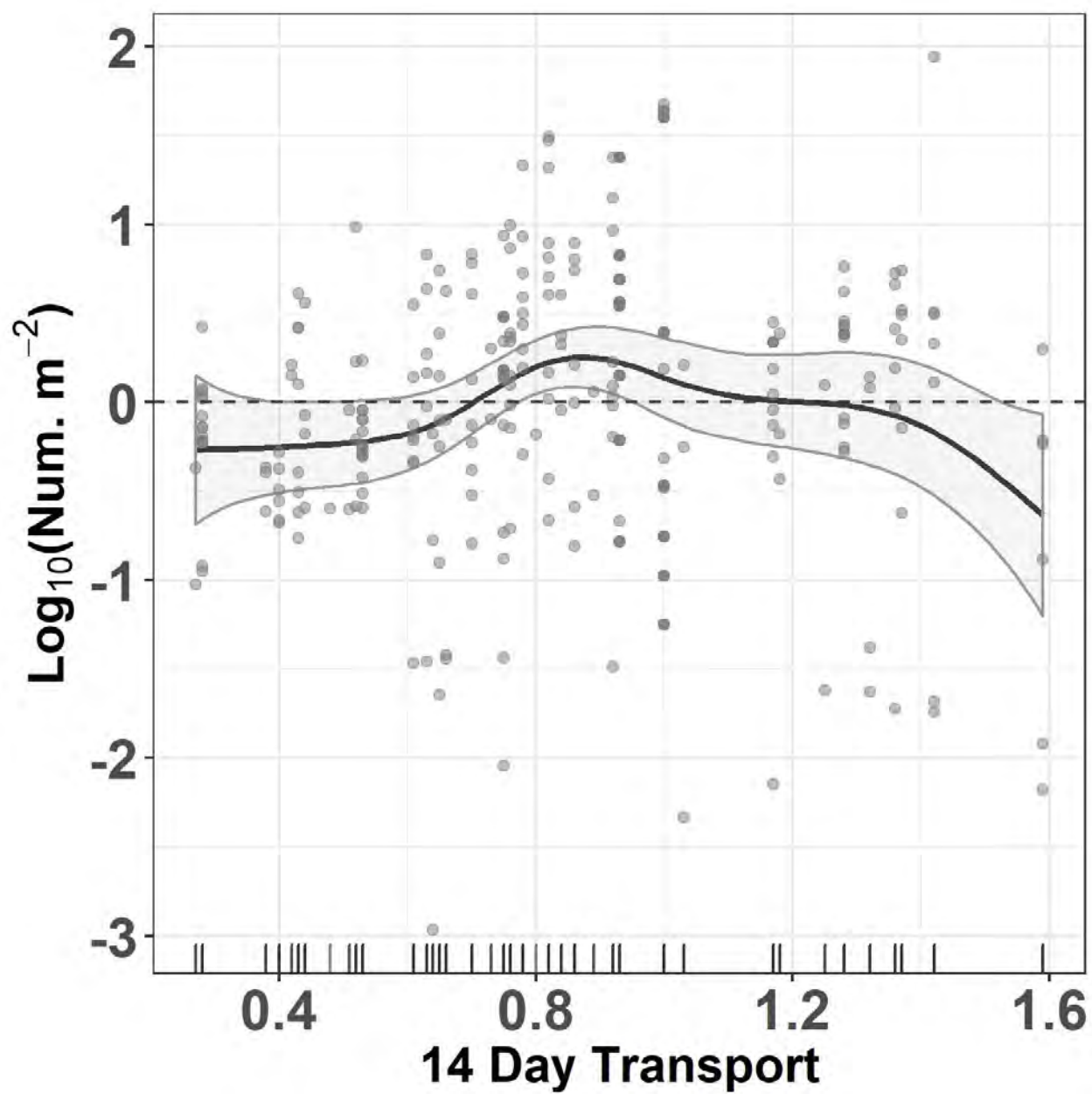


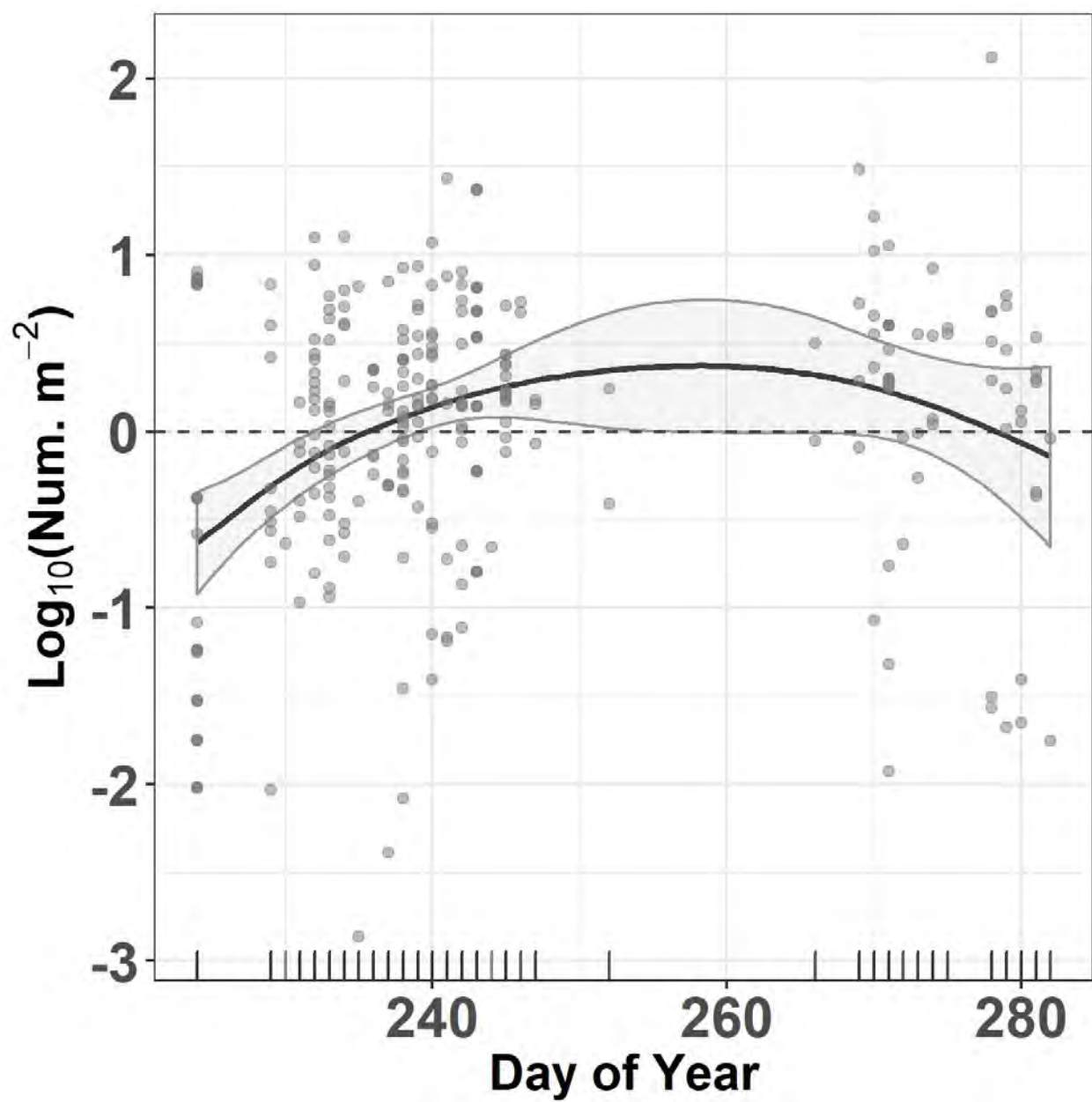


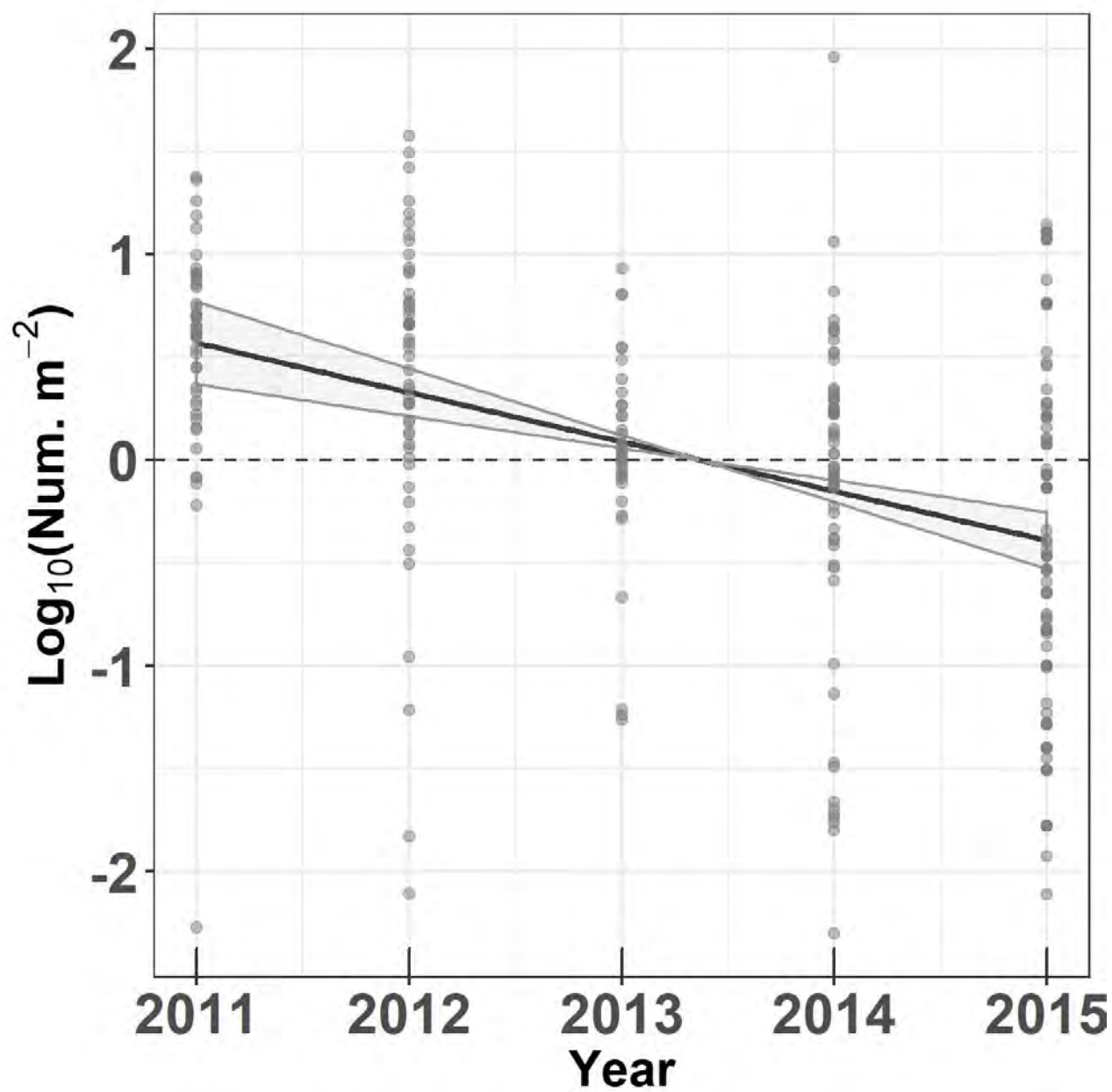


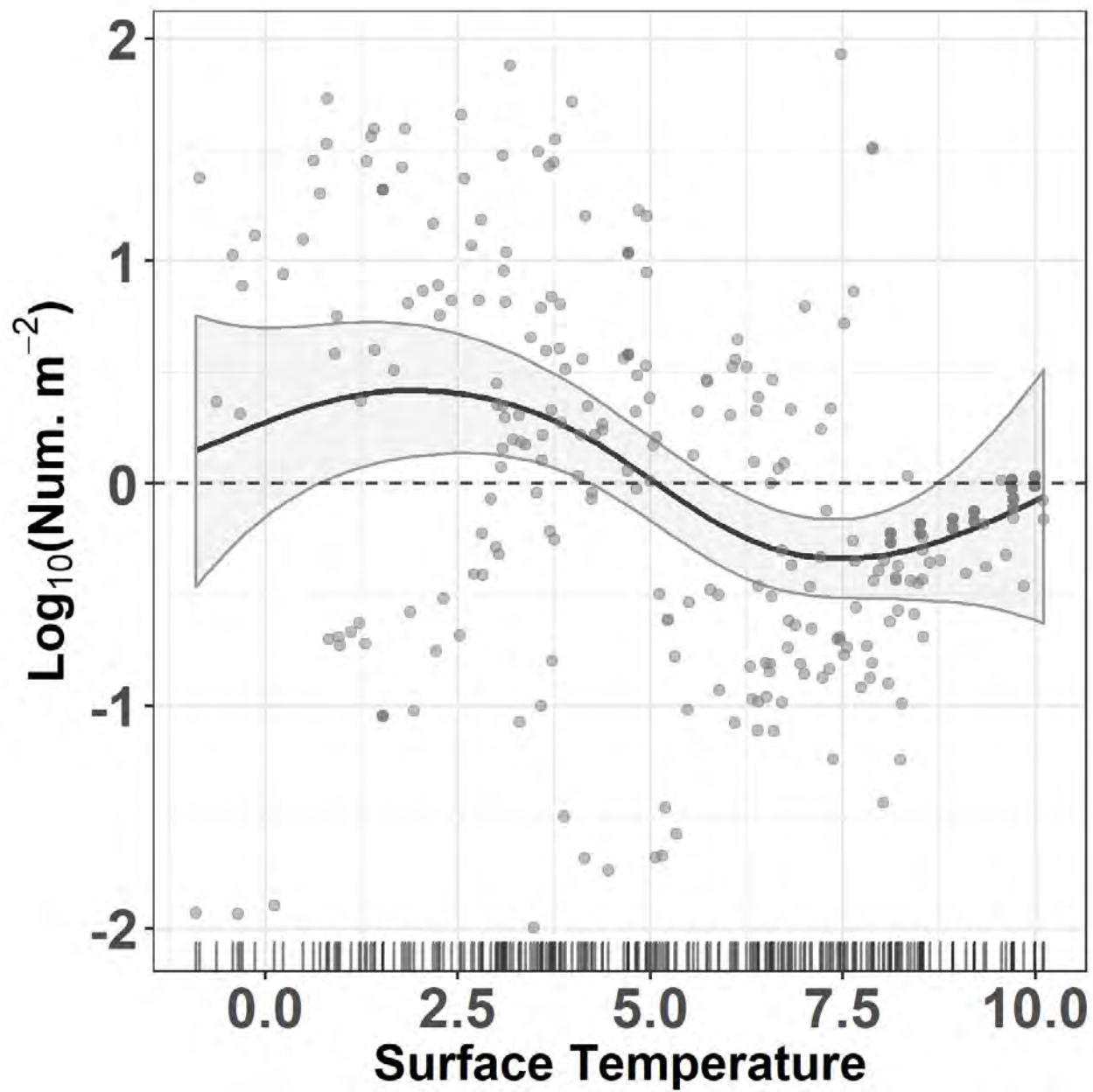


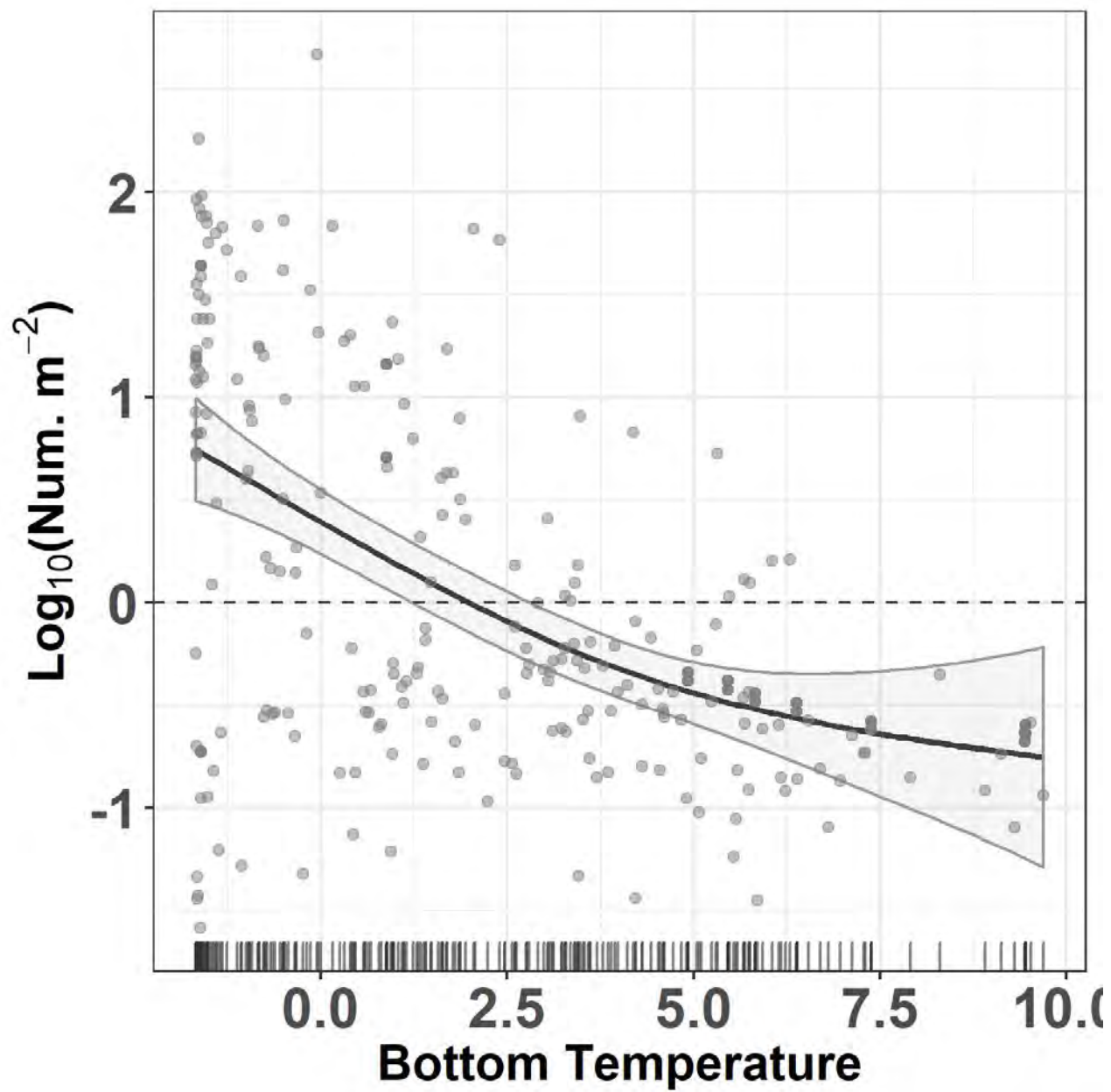


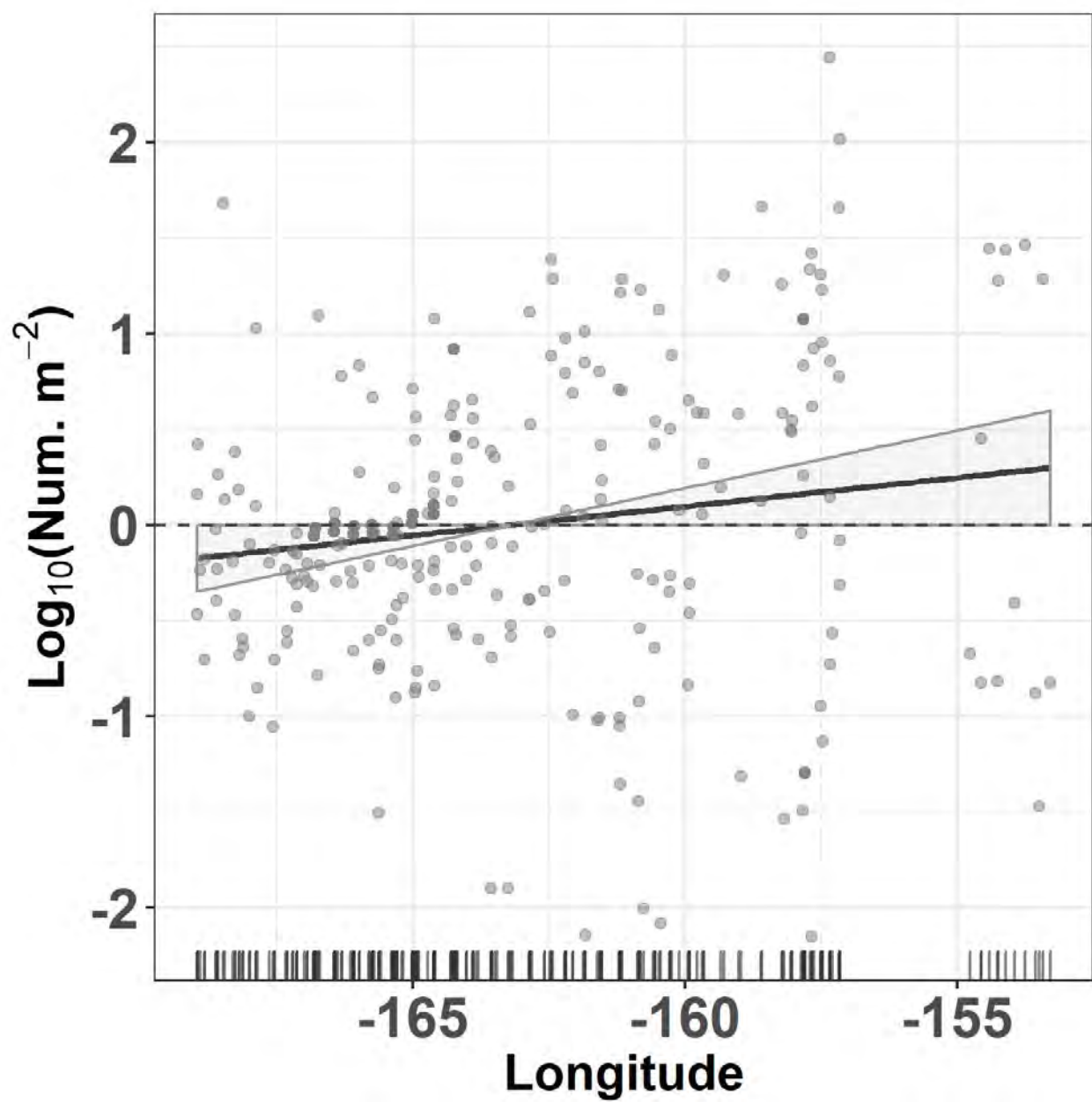


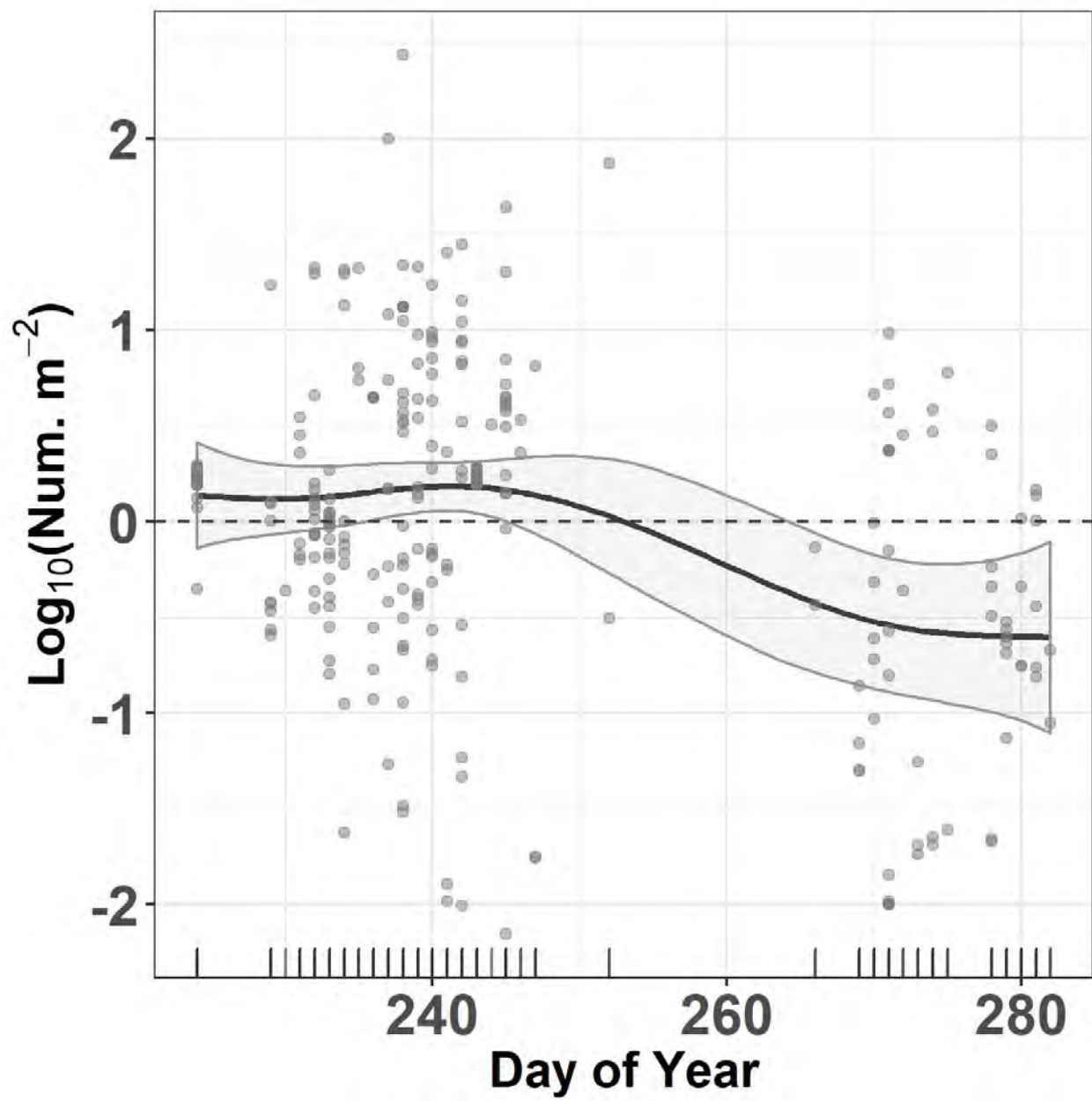


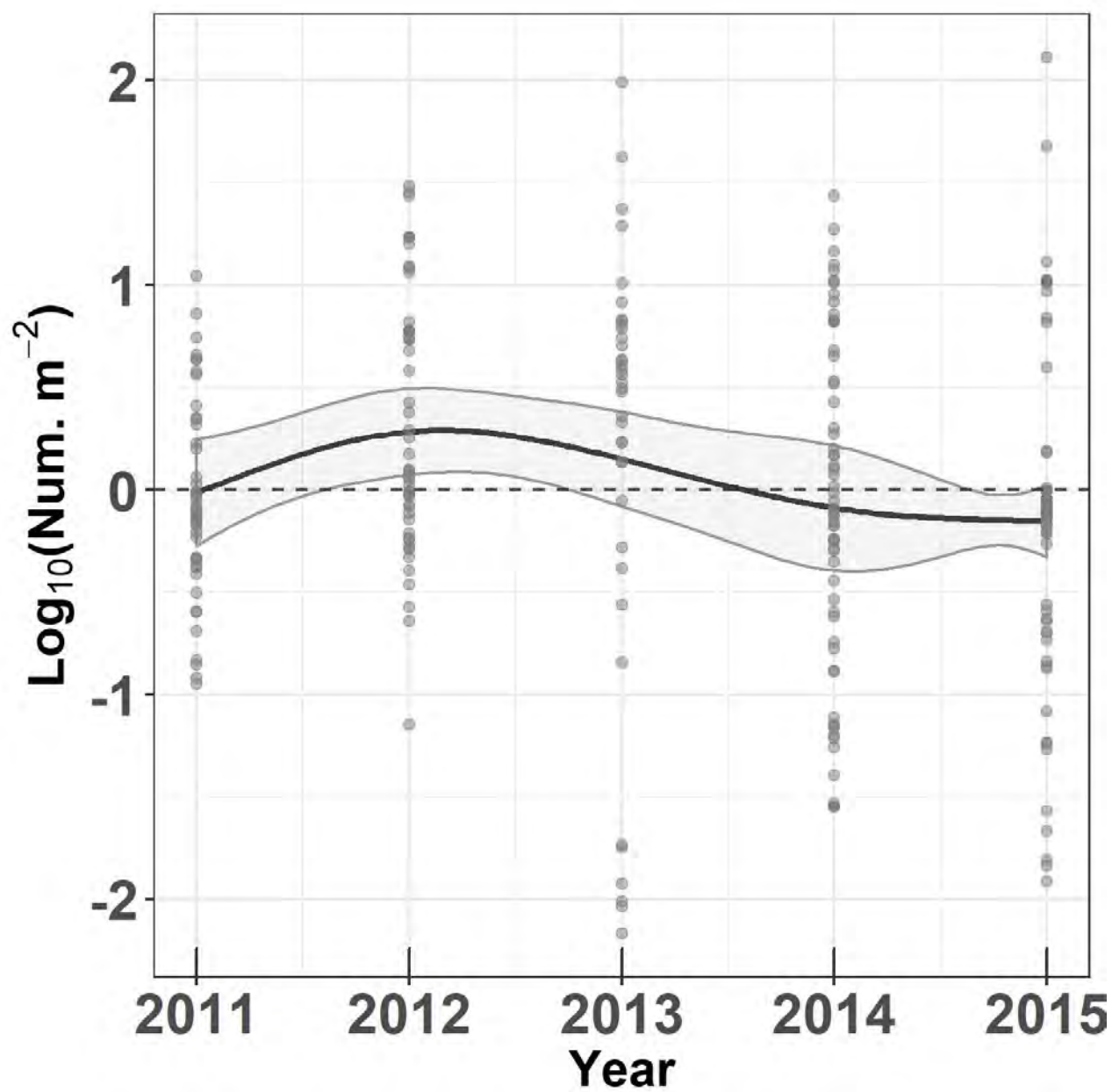












Declaration of interests

The authors declare that they have no known competing financial interests or personal relationships that could have appeared to influence the work reported in this paper.

The authors declare the following financial interests/personal relationships which may be considered as potential competing interests:

Adam Spear: Investigation, Conceptualization, Methodology, Data curation, Formal analysis, Writing - original draft, Visualization. **Jeff Napp:** Investigation, Conceptualization, Methodology, Writing – review and editing, Supervision. **Nissa Ferm:** Data curation, Visualization, Formal analysis. **David Kimmel:** Conceptualization, Methodology, Writing - review & editing.